

Expression profile of pattern recognition receptors in skeletal muscle of SOD1(G93A) ALS mice and sporadic ALS patients.

Sonja Lehmann^{1,4#}, Eliza Esch^{1,#}, Philipp Hartmann¹, Anand Goswami², Stefan Nikolin², Joachim Weis², Cordian Beyer^{1,3} and Sonja Johann^{1,5,CA}

¹ Institute of Neuroanatomy, Medical Clinic RWTH Aachen University, Wendlingweg 2, 52074 Aachen,

² Institute of Neuropathology, Medical Clinic RWTH Aachen University, Pauwelsstraße 30, 52074 Aachen, Germany

³ JARA - Translational Brain Medicine, Aachen, Germany.

⁴ Institute Molecular and Cellular Anatomy (MOCA), Medical Clinic RWTH Aachen University, Wendlingweg 2, 52074 Aachen, Germany

⁵ Institute of Anatomy II, Medical Faculty Heinrich-Heine-University, Moorenstraße 5, 40225, Düsseldorf, Germany

Equal contribution

^{CA} Corresponding author

Sonja Johann, PhD

Phone: 49-(0)241-80-88864

Fax: 49-(0)241-80-82472

Email: Sonja.Johann@med.uni-duesseldorf.de

This article has been accepted for publication and undergone full peer review but has not been through the copyediting, typesetting, pagination and proofreading process, which may lead to differences between this version and the Version of Record. Please cite this article as doi: 10.1111/nan.12483

This article is protected by copyright. All rights reserved.

Keywords: Amyotrophic lateral sclerosis, inflammasomes, caspase 1, IL1 β , NLRC4, NLRP1, AIM2, NLRP3, skeletal muscle

Running title: PRRs expression in the skeletal muscle of ALS animals and patients

List of abbreviations

AD	Alzheimer's disease
AIM2	Absent in melanoma 2
ALS	Amyotrophic lateral sclerosis
ASC	Apoptosis-associated speck-like protein containing a caspase activating and recruitment domain
CARD	Caspase activating and recruitment domain
CNS	Central nervous system
C9ORF72	Chromosome 9 open reading frame 72
DAB	3,3'-Diaminobenzidine
DAMP	Danger associated molecular pattern
fALS	familial ALS
GAPDH	Glyceraldehyde 3-phosphate dehydrogenase
GFAP	Glial fibrillary acidic protein
H&E	Hematoxylin and Eosin
ICE	Interleukin-1 converting enzyme
IL1 β	Interleukin 1 beta
IL18	Interleukin 18

IPAF	ICE-Protease Activating Factor
mROS	mitochondrial reactive oxygen species
MS	Multiple sclerosis
NLR	Nod-like receptor
NLRC4	NLR family CARD domain-containing 4
NLRP1	Nod-like receptor protein 1
NLRP3	Nod-like receptor protein 3
NOD-like	Nucleotide-binding oligomerization domain-like
PBS	Phosphate buffered saline
PCR	Polymerase chain reaction
PRR	Pattern recognition receptor
sALS	Sporadic ALS
SCI	Spinal cord injury
SOD1	Superoxide dismutase 1
TDP43	TAR DNA binding protein
WT	Wild type

Abstract

Aims: Amyotrophic lateral sclerosis (ALS) is characterized by degeneration of motoneurons and progressive muscle wasting. Inflammatory processes, mediated by non-neuronal cells, such as glial cells, are known to contribute to disease progression. Inflammasomes consist of pattern recognition receptors (PPRs), ASC and caspase 1 and are essential for interleukin (IL) processing and a rapid immune response after tissue damage. Recently, we described inflammasome activation in the spinal cord of ALS patients and in SOD1^(G93A) ALS mice. Since pathological changes

in the skeletal muscle are early events in ALS, we hypothesized that PRRs might be abnormally expressed in muscle fibre degeneration.

Methods: Western Blot analysis, real-time PCR and immunohistochemistry were performed with muscle tissue from pre-symptomatic and early-symptomatic male SOD1^(G93A) mice and with muscle biopsies of control and sporadic ALS patients. Analysed PRRs include NLRP1, NLRP3, NLRC4 and AIM2. Additionally, expression levels of ASC, caspase 1, IL1 β and IL18 were evaluated.

Results: Expression of PRRs and ASC was detected in murine and human tissue. The PRR NLRC4, caspase 1 and IL1 β were significantly elevated in denervated muscle of SOD1^(G93A) mice and sALS patients. Furthermore, levels of caspase 1 and IL1 β were already increased in pre-symptomatic animals.

Conclusion: Our findings suggest that increased inflammasome activation may be involved in skeletal muscle pathology in ALS. Furthermore, elevated levels of NLRC4, caspase 1 and IL1 β reflect early changes in the skeletal muscle and may contribute to the denervation process.

Introduction

Amyotrophic lateral sclerosis (ALS) is a progressive neurodegenerative disease, affecting upper and lower motoneurons in the cerebral cortex, brainstem and spinal cord. Leading symptoms are progressive muscle weakness and atrophy, ultimately resulting in paralysis [1]. Respiratory failure is the most common cause of death, usually 3-5 years after the onset of symptoms [2]. About 90% of cases are considered sporadic ALS (sALS), with no obvious risk factors noted [2, 3]. The inherited form of ALS (familial ALS, fALS) accounts for ~10% of all ALS cases and a set of mutant genes is associated with fALS. Currently, the most common fALS mutation is found in chromosome 9 open reading frame 72 (C9orf72, >40%), followed by muta-

tions in the superoxide dismutase 1 (SOD1) gene (approx. 20%) [3-5]. However, it is likely that fALS and sALS share similar pathogenic pathways [6], because clinical symptoms of both forms are indistinguishable [6]. Potential causes such as glutamate excitotoxicity, mitochondrial dysfunction, protein aggregation, and RNA mis-processing [7-13] are believed to contribute to ALS pathogenesis. Additionally, chronic inflammatory processes and activation of the innate immune system are suggested to drive disease progression [14, 15].

As important key players of the innate immune response, inflammasomes have gained focus in recent years. These cytosolic multiprotein complexes consist of a cytoplasmic pattern recognition receptor (PRR), an adaptor protein (apoptosis-associated speck-like protein, ASC) and inflammatory pro-caspase 1 (pro-Casp1) [16-18]. Recognition of damage-associated molecular patterns (DAMPs), including ATP, high-mobility group box 1 (HMGB1), S100 proteins, heat shock proteins and cytosolic DNA, released after cell/tissue damage, can activate the innate immune system [19]. The sensing of DAMPs leads to inflammasome assembly and subsequent activation of pro-Casp1 [17]. Subsequently, active caspase 1 (aCasp1) mediates proteolytic maturation of interleukin 1 β (IL1 β) and interleukin 18 (IL18) [20, 21]. PRRs functioning as inflammasome sensors include the NOD-like receptors NLRP1, NLRP3 and NLRC4 (also known as IPAF, Card12 or CLAN) [22, 23] and the interferon-inducible HIN-200 (hematopoietic interferon-inducible nuclear antigens with 200 amino acid repeats) family member, absent in melanoma 2 (AIM2) [24]. The adaptor protein ASC contains a caspase activating and recruitment domain (CARD) and is required for most inflammasomes [17, 25]. Importantly, NLRP1 and NLRC4 contain a CARD domain which allows them to recruit caspase 1 without the need of ASC [23, 26, 27]. Although it has been reported that ASC binding is essential for efficient autoproteolysis of caspase 1 and cytokine release in CARD-containing inflammasomes, ASC-independent inflammasomes comprise of an unprocessed but active caspase 1 that can initiate rapid cell death [27, 28]. So far, inflammasome activation has been demonstrated in various neurological diseases, including Alzheimer's disease (AD) [29, 30], multiple sclerosis (MS) [31, 32] ischemic stroke [33-35] and spinal cord injury (SCI) [36, 37]. A critical role for caspase 1 and IL1 β in ALS pathogenesis has been demonstrated in animal and cell culture models [38-41]. Re-

cently, we described increased expression of NLRP3, aCasp1, IL1 β and IL18 in the lumbar spinal cord of SOD1^(G93A) mice and in human sALS patients [14, 42].

The neurocentric view of ALS is based on the hypothesis that primary damage occurs in motoneurons and that muscle atrophy is solely the logical consequence of neuronal cell loss [43]. However, it is now evident that non-neuronal cells, such as microglia and astrocytes actively contribute to motoneuron degeneration [8, 43-46]. In this context, it was shown that skeletal muscle-restricted expression of mutant human SOD1 (hSOD1) causes motor neuron degeneration in an ALS mouse model [47], and recent findings suggest that skeletal muscle may actively participate in ALS pathogenesis. Indeed, gene expression changes, increased oxidative stress, impaired protein degradation, defective mitochondrial dynamics and disturbed calcium homeostasis in the skeletal muscle from ALS animal models and human ALS patients were detected early in disease progression [11, 48-54]. Furthermore, activation of inflammatory pathways in the context of tissue remodelling have been described in skeletal muscle of SOD1^(G93A) rats and in human sALS patients [55, 56]. Finally, to provide an early diagnosis for efficient treatment, it is crucial to fully understand muscle pathology in ALS. To further elucidate the role of inflammation in skeletal muscle, we investigated the expression of NLRP1, NLRP3, NLRC4, AIM2 and related inflammasome components and substrates, including ASC, aCasp1 and IL1 β , in pre-symptomatic and early-symptomatic SOD1^(G93A) mice and in human sALS patients.

Material & methods

Animals

All animal experiments were performed according to the guidelines of the Federation of European Laboratory Animal Science Associations and the animal research council and legislation of the district government (North-Rhine Westphalia, Germany). High copy number B6/SJL-Tg (SOD1*G93A)1Gur/J mice [4] carrying a mutant hSOD1 gene, were obtained from Jackson Labs (Stock Number 002726, Bar Harbor, USA). The colony was maintained by crossing B6/SJL males harbouring the SOD1 transgene with wild-type B6/SJL females. All animals were housed in a pathogen

free environment under a 12 hours light/12 hours dark cycle with free access to food and water. Pre-symptomatic male SOD1^{G93A} mice (9 weeks old, SOD1 9W) as well as early symptomatic male SOD1^{G93A} mice (14 weeks old, SOD1 14W) were used to monitor different phases of disease progression. The pre-symptomatic and symptomatic status was defined by analysing motor behaviour of SOD1 mice. Briefly, a neurological score developed for the SOD1 mouse model (ALS therapy development institute, ALSTDI) and accelerating rotarod experiments were performed as described previously [14, 42, 57]. Finally, 14W but not 9W old SOD1 mice exhibited significant motor deficits compared to age-matched male wild type (WT) litters. Genotyping was performed from tail biopsies by a standardized PCR protocol using primers against hSOD1. Furthermore, the transgene copy number of SOD1 animals was determined to exclude artificial effects due to copy number loss. Briefly, genomic DNA was isolated from gastrocnemius muscle using a Tissue DNA Mini Kit (Peqlab, Germany). Real-time PCR was performed using specific primers against human SOD1 and murine IL2. Finally, Δ CT values (Suppl. table S1) were calculated according to the protocol published by Alexander et al. 2004 [58]. Finally, a Δ CT value between 6.6 and 7.2 is thought to result in a stable phenotype.

Mouse tissue collection

Under deep anaesthesia, mice were transcardially perfused with 4% paraformaldehyde in phosphate buffered saline (PBS) (for (immuno)histochemistry) or only with PBS (for protein analysis). The gastrocnemius muscle was dissected and removed. For (immuno-) histochemistry the tissue was post-fixed overnight, embedded in paraffin and cut into 5 μ m cross-sections. For Western Blot analysis, muscle tissue was immediately frozen in liquid nitrogen. Tissues from WT 14W (n=4), SOD1 9W (n=4) and SOD1 14W (n=4) were examined by histology and immunohistochemistry.

Human skeletal muscle biopsies

Human biopsy samples (5 μ m paraffin cross sections and protein lysates in Triton lysis buffer) of skeletal muscle tissue from clinically confirmed, anonymized sALS patients and age-matched controls without neuropathological abnormalities were

obtained from the tissue collection of the Institute of Neuropathology, RWTH Aachen University Hospital, following the guidelines of the Ethics Committee of RWTH Aachen University Hospital. Tissues from control and sALS patients were examined by histology and immunohistochemistry (n=3 controls, n=5 sALS patients) and Western Blot (n=3 controls, n=5 sALS patients).

Hematoxylin/Eosin (HE) staining and Immunohistochemistry

Standard H&E staining was performed to examine muscle structure and histology. Immunohistochemistry was carried out to localize PRRs expression using a standard protocol. Briefly, after deparaffinization, tissue sections were rehydrated followed by subsequent Heat-Induced Epitope Retrieval (HIER) in citrate buffer (pH 6) or Tris-EDTA buffer (pH 9). After blocking of unspecific binding sites using 5% normal serum, sections were incubated with the primary antibody (Suppl. table S3) overnight (ON) at 4°C. The following day, the respective biotinylated secondary antibody was added for 1 hour (h) at room temperature (RT). Immunoreaction was visualized by adding 3,3'-diaminobenzidine (DAB, DAKO, Hamburg, Germany). Nuclei counterstaining was performed using hematoxylin. Negative controls, without primary antibodies, were run simultaneously. Images were taken using the Nikon Eclipse 55i clinical microscope (Nikon, Düsseldorf, Germany) at 20x and 60x magnifications.

To determine the immunoreactive area, colour deconvolution (H DAB) was applied to the RGB pictures (20x magnifications) using ImageJ software. The threshold of the DAB channel was set using an automated routine (Default Red) and the immunoreactive area of the region of interest (ROI) was calculated as percentage of pixels. Sections were viewed using a Leica DMI6000 B inverted microscope

RNA isolation, reverse transcription (RT) and real-time PCR

Gene expression was measured using real-time polymerase chain reaction technology (BioRad, Germany), Sensi Mix™ Plus SYBR Kit (Bioline, UK), and a standardized protocol as described previously. Briefly, isolation of total RNA was performed with TriFast (Peqlab, Germany). RNA samples (1µg) were digested with DNase1

(Roche, Germany) before RT to remove genomic DNA. Reverse transcription was performed using the Invitrogen M-MLV RT-kit and hexanucleotide primers. Samples were analysed in triplets using 96-well plates and the CFX Connect™ Real-Time PCR Detection System (BioRad, Germany). Relative quantification was performed calculating the ratio between the gene of interest (Suppl. table S2) and two reference genes (HSP90 and HPRT) using qBase plus software (qBase Biogazelle, Belgium). In each run, external standard curves were generated by several-fold dilutions of target genes. Finally, data were expressed as fold of WT 9W. Melting curves were routinely performed to determine the specificity of the PCR reaction.

SDS-PAGE and Western blotting

Frozen samples of mouse skeletal muscle were homogenized in Radio-Immunoprecipitation Assay (RIPA) buffer consisting of 150 mM NaCl, 1% (v/v) Nonidet P-40 (Sigma, Igepal, CA), 0.1% SDS (sodium dodecyl sulphate), 0.5% sodium deoxycholate, 50 mM Tris-HCl, pH 8.0 supplemented with 1x protease inhibitor cocktail (1xPi) (Complete Mini, Roche, Germany). Human biopsy material was homogenized in Triton lysis buffer (0.5% Triton X-100 in PBS, 0.5 mM PMSF and 1xPi). The Pierce™ BCA Protein Assay Kit (Thermo Fisher Scientific, Waltham, USA) was used according to the manufacturer's protocol to determine protein concentrations which were measured in a plate reader (Tecan, Infinite 200, Männedorf, Switzerland). Protein samples were separated by 8-12% (v/v) discontinuous sodium dodecyl sulphate-polyacrylamide gel electrophoresis (SDS-PAGE) (BioRad, München, Germany) and transferred to a polyvinylidene difluoride (PVDF) membrane (Roche Diagnostics, Mannheim, Germany). After blocking with 5% skimmed milk (Carl Roth, Karlsruhe, Germany) solved in 0.05% Tween 20/Tris-buffered saline (TBS-T), for 1h at RT, incubation with the primary antibody (Suppl. table S3), diluted in blocking buffer, was performed ON at 4°C. The next day, incubation with the respective HRP-conjugated secondary antibody was executed for 2h at RT. Visualization was performed using enhanced chemiluminescence (ECL plus, Thermo Fisher Scientific, USA). Actin and GAPDH served as loading controls. Densitometric evaluation was executed using ImageJ software (Free Java software provided by the National Institutes of Health, Bethesda, Maryland, USA).

Statistical analysis

Statistical analysis was carried out using SPSS 22 (Chicago, IL) and GraphPad Prism 5.0 (GraphPad Software, San Diego). Parametric statistics were applied with data that met Shapiro-Wilk criteria for normal distribution and passed Bartlett's or Levene's test for equal variances. If necessary, Box-Cox transformation was performed to allow parametric testing. Appropriate results were analysed by unpaired Student's t-test for comparison of mean differences between two groups or one-way ANOVA for multiple comparisons. Data from mature IL1 β protein were analysed by non-parametric Mann-Whitney U test. In case of the mRNA and immunohistochemistry data, two-way ANOVA was performed (with age and genotype as variables). Western Blot and immunohistochemistry for SOD1^(G93A) was performed with WT (n=4) and SOD1 (n=4-5) animals for both time points (9W and 14W); and for tissues of control (n=3) and sALS (n=5) patients. Realtime experiments for WT and SOD1^(G93A) were performed with n=6-7 per group. All data represent the means \pm SEM. Differences were considered significant when $p \leq 0.05$ and exact p-values are given in the result part.

Results

Histopathology of skeletal muscle from SOD1^(G93A) mice and sALS patients

In muscle tissue of 9W old SOD1 animals, morphology was comparable to WT (Figure 1 A, B). In early symptomatic, 14W old SOD1 mice, numerous partially atrophic or atrophic (Figure 1 C, arrows), angular or rounded muscle fibres were found, some of which showed non-subsarcolemmal myonuclei (Figure 1 C, asterisk). In addition, compensatory hypertrophic fibres were detected (Figure 1 C, arrowhead).

Muscle fibres from human control subjects exhibited regular morphology (Figure 1 D), whereas muscle tissues from sALS patients showed numerous groups of partially atrophic and atrophic muscle fibres (Figure 1 E-F, arrows), several hypertrophic muscle fibres (Figure 1 E, arrowhead), and central myonuclei (Figure 1 E, asterisk).

Elevated levels of aCasp1 and IL1 β in skeletal muscle of SOD1^(G93A) mice and sALS patients

Inflammasome formation leads to auto-proteolysis and activation of pro-Casp1, and cleavage of pro-IL1 β and -IL18 into their active forms [18]. Thus, expression levels of Casp1, IL1 β and IL18 were analysed by Western blotting (Figure 2). Pro-Casp1 and pro-IL1 β were expressed in mice and in human patients. Levels of pro-IL1 β remained unchanged in SOD1 animals (Figure 2 A-B, G, I) whereas expression of pro-Casp1 was significantly upregulated in 14W (Figure 2 A-B, E * $p=0.0407$) but not in 9W (Figure 2 A-C) old SOD1 mice. Significantly increased levels of aCasp1 (Figure 2 A-B, D ** $p=0.0022$ and Figure 2F * $p=0.0103$) and mature IL1 β (Figure 2 H, * $p=0.0159$ and Figure 2 J, * $p=0.0159$) but not mature IL18 (Figure 2 L, N) were detected in SOD1 animals of both ages. Levels of pro-IL18 remained unchanged in SOD1^(G93A) mice (Figure 2 K, M).

In human (Figure 2 O-Q), the 35-kDa subunit of pro-Casp1 (Figure 2 P ** $p=0.0095$) and pro IL1 β (Figure 2 Q ** $p=0.0089$) were significantly elevated in sALS patients. However, aCasp1 and mature IL1 β were not detected in human samples (Figure 2 O). Neither pro- nor mature IL18 were detected in human samples (Figure 2 O).

Protein and mRNA expression of inflammasome components in SOD1^(G93A) mice

Next, the expression and regulation of PRRs in the skeletal muscle of pre-symptomatic and symptomatic SOD1^(G93A) mice was examined (Figures 3 and 4). With respect to NLRP1, two immunoreactive bands were detected by Western blotting: a product with a molecular mass of approx. 165 kDa, expected to be the canonical isoform, and a smaller product of approx. 15 kDa, presumably a proteolytic product. Both proteins were found in WT and SOD1 mice (Figure 3 A and 4 A). A significant downregulation of the 165-kDa canonical isoform was detected in 14W (Figure 4 A-B * $p=0.0351$) but not 9W old SOD1 mice (Figure 3 A-B). Expression levels of the 15-kDa product were constant at both ages and in both genotypes (Figures 3 A, C and 4 A, C). Three immunoreactive bands were detected for NLRC4: the full-size canonical 116-kDa and two smaller proteins, of approx. 40 kDa and 18 kDa (Figures 3 A and 4 A). All three products were expressed at detectable levels in 14W old WT

and SOD1 animals (Figure 4A, D-F). Expression levels of all three NLRC4 products (Figure 4 A, 4 D * $p=0.0469$, 4 E ** $p=0.0045$ and 4 F ** $p=0.0015$) were significantly elevated in 14W old SOD1 mice. In 9W old animals, only the 40- and 18-kDa products of NLRC4 were detected (Figure 3 A, D-E), with a significant increase of the 18-kDa product (Figure 3E ** $p=0.0040$). Protein levels of NLRP3 were not significantly different between 9W (Figure 3 A, F) and 14W old WT and SOD1 animals (Figure 4 A, G). One single band, with a molecular weight of approximately 50 kDa, was observed for AIM2 in WT and SOD1 mice (Figures 3 A and 4 A). Compared to WT, AIM2 protein levels were significantly elevated in 14W (Figure 4 H * $p=0.0188$) but not 9W old SOD1 animals (Figure 3 G). Expression levels of ASC were very low in skeletal muscle of WT and SOD1 mice (Figures 3 A and 4 A). Beside the expected 22-kDa ASC monomer, we detected a product of approximately 35 kDa, which is, to our knowledge, not reported in the literature. Quantification of the 22 and 35 kDa products revealed no significant differences between WT and SOD1 of 9W (Figure 3 A, H) and 14W old mice (Figure 4 A, I).

In a next step, we examined mRNA expression of PRRs, ASC and interleukins (Figure 5). Specific transcripts of all investigated PRRs (Figure 5 A-D) were detected in WT and SOD1 muscle. A significant interaction (age*genotype * $p=0.0180$) was detected for NLRC4. Simple main effects analysis revealed a significant reduction of NLRC4 mRNA in 9W old SOD1 mice (Figure 5 B * $p=0.0195$). Expression levels of remaining PRRs were not altered (Figure 5 A, C-D). No interaction but an age dependent downregulation of ASC (Figure 5 E ** $p=0.0021$) and IL18 mRNA (Figure 5 F ** $p=0.0006$) was found in 14W old SOD1 mice. Transcription levels of IL1 β were not significantly altered (Figure 5 G).

Subcellular localization of inflammasome components in the skeletal muscle of SOD1^(G93A) mice

Immunohistochemistry was performed to depict the cellular localization of inflammasome components (Figure 6). A weak intermyofibrillar staining pattern of NLRP1 was detected in WT and SOD1 animals, in which some fibres exhibited a stronger staining than others (Figure 6 A-C; inset, asterisks). Myonuclei were negative for NLRP1 (Figure 6 A-C). No visible differences were observed between WT

and 9W SOD1 (Figure 6 A-B). Staining intensity of NLRP1 appeared slightly weaker in 14W old SOD1 mice (Figure 6 C). However, the immunoreactive area was not significantly different in SOD1 mice of both ages (Figure 6 D). NLRC4 displayed a diffuse intermyofibrillar (Figure 6 E-G; inset, asterisks) and subsarcolemmal (Figure 6 G; inset, white arrowhead) expression pattern in both genotypes. Interestingly, a prominent immunoreactivity of NLRC4 was observed within the myonucleus/myonuclear domain (Figure 6 F-G, inset, black arrowhead). Furthermore, a significant interaction (age*genotype **p=0.0051) was detected. Analysis of simple main effects revealed that age significantly affects NLRC4 immunoreactivity (Figure 6 H **p=0.0066). As expected, NLRP3 immunoreactivity was faint in WT and SOD1 muscle (Figure 6 I-K). However, some muscle fibres displayed a diffuse intermyofibrillar and myonuclear NLRP3 staining pattern (Figure 6 I-K; inset, asterisks and black arrowheads, respectively). Importantly, isolated cells between muscle fibres, most likely macrophages, exhibited a strong NLRP3 immunoreactivity (Figure 6 K, black arrowhead). Nevertheless, no differences in NLRP3 immunoreactivity were observed (Figure 6 L). AIM2 was mainly localized within the myonucleus/myonuclear domain (Figure 6 M-O; inset, black arrowheads) and less expressed in the intermyofibrillar compartment (Figure 6 M-O; inset, asterisks). The immunoreactive area was not significantly different in SOD1 mice (Figure 6 P). ASC displayed a strong subsarcolemmal staining pattern in single muscle fibres of WT and SOD1 animals (Figure 6 Q-S; inset, white arrowheads). In 14W SOD1, ASC immunoreactivity was detected near the plasma membrane of isolated muscle fibres (Figure 6 S; inset, white arrowhead), whereas most fibres rarely gave any positive signal (Figure 6 Q-S, black asterisks).

Elevated levels of PRRs and ASC in muscle biopsies from sALS patients

Western Blot analysis was performed with control (n=3) and sALS tissue (n=5). Both, the full-size 165-kDa NLRP1 and the smaller 15-kDa fragment were detected in control and sALS patients (Figure 7 A). No significant differences in the expression level of both protein variants were observed (Figure 7 B-C). Consistent with data from the mouse model, the expression level of NLRC4 was increased in sALS patients (Figure 7 A, D-E). Statistical differences were detected for the 18-kDa (Figure 7 E

* $p=0.0307$) but not for the 116-kDa, canonical isoform (Figure 7 D $p=0.0956$). Due to no detectable expression of the 40-kDa isoform in controls, a reliable quantification was not feasible (Figure 7 A). Protein levels of the 118-kDa canonical NLRP3 isoform were below the detection limit in control and sALS patients (Figure 7 A). Expression of the 50-kDa AIM2 protein was similar in control and sALS patients (Figure 7 A, F). The 22-kDa ASC monomer was not detected in any of the samples (Figure 6 A). However, the 35-kDa product was expressed but not statistically different in sALS patients (Figure 7 A, G $p=0.5233$).

Immunohistochemistry of NLRP1 revealed intermyofibrillar localization (Figure 8 A-C; inset, asterisks). In sALS patients, isolated atrophic fibres displayed a stronger signal than normal sized and hypertrophic muscle cells (Figure 8 B-C; inset, asterisks). However, the immunoreactive area was not significantly different in sALS patients (Figure 8 D). Expression of NLRC4 was mainly localized within/around myonuclei (Figure 8 E-G; inset, black arrowheads) and to a lesser extent in the intermyofibrillar compartment (Figure 8 F-G; inset, asterisks). A prominent staining of atrophic muscle fibres was detected in sALS samples (Figure 8 F-G). Finally, the immunoreactive area was significantly increased in sALS patients (Figure 8 H). Immunostaining of NLRP3 (Figure 8 I-K) and AIM2 (Figure 8 M-O) was faint and localized in the intermyofibrillar compartment (Figure 8 I-O; inset, asterisks) and to a lesser extent in the nucleoplasm (Figure 8 I-O; inset, black arrowheads) of control and sALS patients. We observed no significant differences between control and sALS in either the NLRP3 (Figure 8 L) or AIM2 staining (Figure 8 P). A weak signal of ASC was detected in intermyofibrillar compartment (Figure 8 Q-S; inset, asterisks) of control and sALS subjects. However, evaluation of the immunoreactive area did not reveal a statistical difference (Figure 8 T).

Importantly, some cells (most likely macrophages and/or endothelial cells) located between muscle fibres exhibited a strong immunoreactivity for NLRC4, NLRP3, AIM2 and ASC (Figure 8 E-S, black arrows).

Discussion

Activation of the innate immune system is a known mechanism in neurodegeneration and activation of inflammasomes has been demonstrated in various neurological diseases [59-61]. We recently demonstrated increased expression of NLRP3, aCasp1 and IL1 β in the spinal cord of SOD1^(G93A) mice and sALS patients [14]. Furthermore, blocking of inflammasome signalling exerts neuroprotective effects in SCI [36, 37], ischemic stroke [33, 62], MS [63], AD [64] and ALS [39]. However, expression of inflammasomes in normal and denervated skeletal muscle in ALS is largely unknown. Thus, we aimed to determine the expression of the PRRs NLRP1, NLRP3, NLRC4, AIM2 and other inflammasome components, such as ASC, caspase 1 and IL1 β /18 in the SOD1^(G93A) mouse model and in sALS patients. Elevated levels of caspase 1 and IL1 β in SOD1 mice and sALS patients indicate inflammasome activation in the denervated skeletal muscle. Moreover, increased levels of these proteins in the skeletal muscle of pre-symptomatic SOD1 animals suggest an early activation of innate immunity in ALS pathogenesis. NLRP3 and ASC were expressed at very low, but detectable levels. However, no significant differences in protein expression were detected. NLRP1 was downregulated in SOD1^(G93A) mice but not in human sALS patients. Protein expression of NLRC4 and AIM2 was increased in symptomatic animals, whereas only NLRC4 was significantly up-regulated in sALS patients. Finally, despite a significant decrease of ASC and IL18 mRNA in 14W old SOD1 animals, no changes in gene expression were detected.

Skeletal muscle is increasingly considered as an active player in ALS pathogenesis by activating retrograde signalling mechanisms, contributing to motoneuron death [65-67]. Thus, early abnormalities in skeletal muscle metabolism may be a primary pathophysiological event in ALS [11, 48, 54, 68-71]. Recent findings, that skeletal muscle fibres express different PRRs, including diverse TLRs and NLRs point out the possibility of a response to environmental factors, including pathogens, inflammatory cytokines and growth factors [72-75]. Caspase 1 and IL1 β have been shown to play a crucial role in disease progression in ALS mice and deficiency in either casp1 or IL1 β , or treatment with the IL1R-antagonist Anakinra reduced neuroinflammation and prolonged the live span of the animals [38-40, 76]. IL1 β can be released by skeletal muscle cells [77] and/or by macrophages, which infiltrate the

diseased skeletal muscle [78]. Elevated level of IL1 β and IL18 seem to be involved in the initiation and progression of idiopathic inflammatory myopathies, including dermatomyositis, polymyositis and inclusion body myositis [79, 80]. Furthermore, primary skeletal muscle cells release IL1 β after treatment with lipopolysaccharide (LPS) and ATP, suggesting that skeletal muscle may actively participate in inflammasome formation [81]. During muscle regeneration, increased IL1 β is associated with an accumulation of activated macrophages and impaired regeneration [78]. Our observation of increased mature IL1 β is in accordance with a recent study on Schwann cell and macrophage mediated inflammation in the skeletal muscle, performed in SOD1^(G93A) transgenic rats [56]. Additionally, we detected elevated levels of aCasp1, the rate-limiting enzyme in cytokine maturation, in 9W and 14W old SOD1^(G93A) mice. These findings are in accordance with a previous study [82], demonstrating increased caspase 1 and 3 activation in the soleus muscle of end-stage but not pre-symptomatic SOD1^(G93A) mice. However, the soleus muscle is mainly composed of slow twitch (Type I) fibres and is therefore later affected in disease progression than the gastrocnemius muscle (predominately type II fast twitch fibres) [68]. On the transcriptional level we detected a significant reduction of IL18 mRNA in 14W old SOD1 mice, whereas transcription levels of IL1 β remained unchanged. Regulation of IL18 and IL1 β may occur on the transcriptional and/or post-translational level. We observed constitutive expression of mRNA and protein of ILs precursors in WT and SOD1 animals. Thus, increased levels of mature IL1 β may be rather derived by posttranslational modification (e.g. increased caspase 1 activity) than by enhanced transcription. So far, we do not have a satisfactory explanation for the decrease in IL18 mRNA expression. However, distinct regulation of IL18 and IL1 β on the transcriptional level, processing and secretion has been described [83]. Given that IL18 has been shown to affect lipid metabolism in skeletal muscle [84-86], decreased levels of IL18 may negatively impact muscle physiology. Thus, reduced IL18 level in denervated skeletal muscle may further contribute to muscle wasting in SOD1 mice. Despite a significant up-regulation of the pro-Casp1 and IL1 β , the mature proteins, were not detected in human samples. Furthermore, protein expression of IL18 was under the detection limit. So far, we don't have a satisfactory explanation, but critical points might be low antibody specificity to the human mature proteins and/or short half-life of the peptides [87]. It has been proposed that NLRP3 may ex-

ert a key role in triggering insulin resistance in obese patients, sarcopenia in aging subjects [88, 89], dysferlin-related dystrophies [81] and sepsis-induced muscle atrophy [90]. Furthermore, it has been shown that the gastrocnemius muscle is capable of up-regulating NLRP3 and IL1 β mRNA in response to sepsis [90]. Although protein expression was low, we detected NLRP3 positive cells in the skeletal muscle of WT and SOD1 mice. However, mRNA and protein expression of NLRP3 were not significantly different in SOD1 animals. In human, NLRP3 protein expression was below the detection limit of Western Blot analysis, but isolated NLRP3 positive cells were found in the connective tissue of the skeletal muscle from murine and human samples. These cells are most likely inflammatory cells, such as macrophages, phagocytosing and/or repairing degenerating muscle fibres and NMJs [55, 56]. Our data are in accordance with other studies demonstrating low expression levels of NLRP3 in normal skeletal muscle [81]. Increased levels of IL1 β and casp1 but weak expression of NLRP3 indicates that rather different PRRs (e.g. NLRP1, NLRC4 or AIM2) may be activated in the skeletal muscle. In 2009, AIM2 was identified a sensor for cytoplasmic DNA, leading to activation of caspase-1 [24, 91-93]. We detected increased protein expression of AIM2 in 14W old SOD1 mice but not in sALS patients. However, expression levels of AIM2 mRNA were not significantly altered in SOD1 mice. These findings suggest a regulation of AIM2 on the posttranslational level by mechanisms, such as impaired autophagy [54, 94, 95]. Although known to be a predominantly cytosolic localized protein [91], we observed AIM2 immunoreactivity in the nucleoplasm and in cells others than muscle fibres (most likely macrophages). However, our findings are in accordance with recent studies on the role of AIM2 in DNA damage after radiation [96] and neuronal pyroptosis after infection and traumatic brain injury [97].

An extensive diversification of NLRP1 between mouse and human resulted in three paralogues (NLRP1 a,b,c with a similar kDa size) in mice and only one known paralogue (NLRP1) in human. Furthermore, several splice variants have been documented for NLRP1b [98]. NLRP1a and NLRP1b are translated into proteins with a similar molecular weight, whereas NLRP1c is predicted to be a pseudogene. The NLRP1c paralogue does not encode for a full-length inflammasome sensor, but it is truncated after exon 8 [98]. The antibody used in the present study detects endogenous level of total NLRP1 protein. Specific antibodies, only detecting one paralogue,

were not available at the time of this study. We detected two immunoreactive NLRP1 products in mouse and human samples. The 165-kDa protein (NLRP1a and/or b) was significantly downregulated in SOD1^(G93A) mice, whereas expression of the 15-kDa variant was unchanged. No isoform with a size of 15-kDa is known, but there are reasonable grounds to believe that it is the result of a proteolytic event. However, nonspecific reactivity of the used antibody cannot be ruled out. Because the NLRP1b locus is most frequently associated with inflammasome formation, we have analysed mRNA expression of this specific isoform in SOD1^(G93A) mice [99]. In addition, it is not clear what stimuli might specifically activate NLRP1a. Nevertheless, a previous study identified a missense gain-of-function mutation in NLRP1a (Q593P) that exhibits spontaneous inflammasome activation [100]. However, no changes on the mRNA level of NLRP1b were observed. Western Blot analysis of NLRP1 in human control and sALS patients was similar but without significant differences in the expression level. In addition to sensing microbial stimuli, NLRP1 has been suggested to detect metabolic disturbances [101-103]. Autocatalytic cleavage within the FIIND domain (function to find) of NLRP1 occurs constitutively, prior to activation signals, and is required for inflammasome activity [104-106]. Furthermore, it has been published that proteolytic processing of human NLRP1 and mouse NLRP1b results in multiple C-terminally truncated variants [105, 107], including products with the size of approximately 15 kDa [108, 109]. Immunohistochemistry revealed an intermyofibrillar localization of NLRP1 in isolated muscle fibres. This staining pattern was found in control and ALS tissue of mice and human, probably reflecting differences in protein synthesis in different fibre types [110]. However, no differences in the immunoreactive area were detected for NLRP1. In case of NLRC4, we detected a significant upregulation of NLRC4 in symptomatic SOD1^(G93A) mice and in sALS patients. NLRC4 is mainly regarded as a sensor of microbial flagellins [111, 112], but NLRC4 activation was also reported in mouse models for MS [113], acute brain injury [114], and alcohol-induced liver injury [115], suggesting that other, so far unknown, host molecules can activate the NLRC4 inflammasome. Four different isoforms (isoform 1: 116 kDa, isoform 2: 40 kDa, isoform 4: 18 kDa and isoform 4: 10kDa), produced by alternative splicing, have been predicted in human [116] (UniProtKB-Q9NPP4 (NLRC4_HUMAN)). In mice, only the canonical 116-kDa isoform 1 has been described so far (UniProtKB - Q3UP24 (NLRC4_MOUSE)). We detected the expression of the 116-kDa, 40- and 18-kDa NLRC4 isoforms (isoform 1-3) in SOD1^(G93A)

mice and sALS patients. No further information is currently available about the functional role of the small non-canonical isoforms (isoform 2-4) and proteolytic processing of NLRC4. However, nonspecific reactivity of the used antibody cannot be ruled out. In a recent study Schieber and co-workers demonstrated that gut colonization of mice by a strain of *Escherichia coli* prevented *Salmonella* induced muscle wasting [117]. Using knockout mice for Casp1, NLRC4, IL1 β and IL18 they have further confirmed that this effect was NLRC4 and IL18 dependent. Additionally, increased IL18 levels correlated with elevated serum IGF1 and reduced muscle wasting in *Salmonella* infected mice. Together, these data suggest a possible protective effect of NLRC4 activation and IL18 release on skeletal muscle metabolism.

The adaptor protein ASC was expressed at very low levels and co-localization with skeletal muscle fibres was weak in murine and human samples. Furthermore, we detected a strong immunoreactive band, with a size of about 35 kDa in murine and human samples. Although no isoform with the indicated size has been described so far, a recent study on inflammasome activation in prostate cancer detected a product about 30 kDa for ASC in different cancer cell lines [118]. However, nonspecific reactivity of the antibody cannot be ruled out. ASC immunoreactivity was most prominent near the plasma membrane of some muscle fibres and in cells other than muscle fibres. Macrophages are located within the connective tissue and known to express most inflammasome components, including ASC [119].

Although responsible for muscle regeneration after injury, chronic activation of macrophages may exacerbate secondary damage to the denervated skeletal muscle.

Increased infiltration of immune and inflammatory cells (e.g. macrophages, neutrophils, lymphocytes etc.) in the skeletal muscle, early in disease progression, has been documented in ALS animal models [56, 120, 121] and in a subset of sALS patients [122, 123]. Importantly, increased expression levels of inflammasome components might be, at least in part, due to the infiltration of immunocompetent cells into the muscle tissue due to muscle fibre necrosis [123]. Additionally, other cell types, including fibroblasts, Schwann cells, endothelial cells, and satellite cells may also express and upregulate different NLRs. However, these cell types account for only a tiny proportion in the analysed samples and our data most likely reflect changes in skeletal muscle fibres.

Importantly, since mRNA expression of PPRs and IL1 β was hardly unchanged in 9 and 14W old SOD1 mice, the observed changes appear to be the results of post-transcriptional and/or posttranslational events [124-128]. However, artefacts due to hSOD1 copy number loss can be largely excluded since Δ CT values were within the predicted range [58]. Thus, future studies on mouse and human sALS skeletal muscle samples are needed to clarify these points.

Limitations and conclusion

We are aware that the present study has some limitations. With the background of a heterogeneous and multifactorial disease, the small number of samples limits the ability to generalize our data. However, major advantages of our study are the detailed expression analysis of major inflammasome components in normal and denervated skeletal muscle from a genetic mouse model for ALS and sALS patients. To our knowledge, this is the first study investigating protein expression of NLRP1, NLRP3, NLRC4 and AIM2 in normal and denervated skeletal muscle. Whether this expression pattern is specific for ALS or might be similar in other neurogenic muscle atrophies, due to sensorimotor neuropathy, remains to be investigated. Our results from the SOD1^(G93A) mouse model suggest that activation of the innate immune system in denervated skeletal muscle is an early event and may actively contribute to muscle wasting and disease progression. Especially NLRC4 protein expression was significantly changed in the mouse model and in sALS patients, suggesting a possible role in skeletal muscle pathology. Although the relative contribution of inflammasome activation merits further investigation, our findings may contribute to a better understanding how inflammatory processes may contribute to denervation processes and muscle atrophy in ALS.

Conflict of interest

The authors declare no competing interests.

Acknowledgements

We would like to thank U. Zahn, H. Helten and P. Ibold (Institute of Neuroanatomy, RWTH Aachen University) as well as A. Knischewski (Institute of Neuropathology, RWTH Aachen University) for their excellent technical support. This work was supported by a grant of the RWTH Aachen University (START, S.J.).

Author Contributions

S.L. and E.E. performed the HE stains, immunohistochemistry and Western Blot analysis of human control and sALS samples. S.L. and E.E. also executed immunostaining and Western blotting for NLRP1, NLRC4, AIM2, IL18 and B8H10 in SOD1^(G93A) mouse samples. P.H. performed Western Blot analysis and immunohistochemistry for NLRP3, ASC, caspase 1 and IL1 β for the SOD1^(G93A) mouse samples. P.H. and S.J performed mRNA extraction, cDNA synthesis and real-time PCR analysis. S.J and S.L performed DNA extraction and copy number analysis. S.J. was responsible for animal experiments and tissue collection from SOD1^(G93A) mice. S.L., E.E. and S.J. wrote the manuscript. Skeletal muscle biopsies of control and sALS cases were sampled and processed by S.N, J.W. and A.G. S.J. raised the hypothesis and designed the experiments. Statistics was carried out by S.J, S.L., E.E and P.H. The entire project was supervised by S.J. and C.B.

References

- 1 Kiernan MC, Vucic S, Cheah BC, Turner MR, Eisen A, Hardiman O, Burrell JR, Zoing MC. Amyotrophic lateral sclerosis. *Lancet (London, England)* 2011 Mar 12; **377**: 942-55
- 2 Salameh JS, Brown RH, Jr., Berry JD. Amyotrophic Lateral Sclerosis: Review. *Seminars in neurology* 2015 Aug; **35**: 469-76
- 3 Gitler AD, Tsuiji H. There has been an awakening: Emerging mechanisms of C9orf72 mutations in FTD/ALS. *Brain research* 2016 Sep 15; **1647**: 19-29
- 4 Gurney ME, Pu H, Chiu AY, Dal Canto MC, Polchow CY, Alexander DD, Caliendo J, Hentati A, Kwon YW, Deng HX, et al. Motor neuron degeneration in mice that express a human Cu,Zn superoxide dismutase mutation. *Science (New York, NY)* 1994 Jun 17; **264**: 1772-5

- 5 Ince PG, Highley JR, Kirby J, Wharton SB, Takahashi H, Strong MJ, Shaw PJ. Molecular pathology and genetic advances in amyotrophic lateral sclerosis: an emerging molecular pathway and the significance of glial pathology. *Acta neuropathologica* 2011 Dec; **122**: 657-71
- 6 Gros-Louis F, Gaspar C, Rouleau GA. Genetics of familial and sporadic amyotrophic lateral sclerosis. *Biochimica et biophysica acta* 2006 Nov-Dec; **1762**: 956-72
- 7 Alami NH, Smith RB, Carrasco MA, Williams LA, Winborn CS, Han SS, Kiskinis E, Winborn B, Freibaum BD, Kanagaraj A, Clare AJ, Badders NM, Bilican B, Chaum E, Chandran S, Shaw CE, Eggan KC, Maniatis T, Taylor JP. Axonal transport of TDP-43 mRNA granules is impaired by ALS-causing mutations. *Neuron* 2014 Feb 05; **81**: 536-43
- 8 Boillee S, Vande Velde C, Cleveland DW. ALS: a disease of motor neurons and their nonneuronal neighbors. *Neuron* 2006 Oct 05; **52**: 39-59
- 9 Cozzolino M, Carri MT. Mitochondrial dysfunction in ALS. *Progress in neurobiology* 2012 May; **97**: 54-66
- 10 Evans MC, Couch Y, Sibson N, Turner MR. Inflammation and neurovascular changes in amyotrophic lateral sclerosis. *Molecular and cellular neurosciences* 2013 Mar; **53**: 34-41
- 11 Goswami A, Jesse CM, Chandrasekar A, Bushuven E, Vollrath JT, Dreser A, Katona I, Beyer C, Johann S, Feller AC, Grond M, Wagner S, Nikolin S, Troost D, Weis J. Accumulation of STIM1 is associated with the degenerative muscle fibre phenotype in ALS and other neurogenic atrophies. *Neuropathology and applied neurobiology* 2015 Apr; **41**: 304-18
- 12 Prause J, Goswami A, Katona I, Roos A, Schnizler M, Bushuven E, Dreier A, Buchkremer S, Johann S, Beyer C, Deschauer M, Troost D, Weis J. Altered localization, abnormal modification and loss of function of Sigma receptor-1 in amyotrophic lateral sclerosis. *Human molecular genetics* 2013 Apr 15; **22**: 1581-600
- 13 Turner MR, Bowser R, Bruijn L, Dupuis L, Ludolph A, McGrath M, Manfredi G, Maragakis N, Miller RG, Pullman SL, Rutkove SB, Shaw PJ, Shefner J, Fischbeck KH. Mechanisms, models and biomarkers in amyotrophic lateral sclerosis. *Amyotrophic lateral sclerosis & frontotemporal degeneration* 2013 May; **14 Suppl 1**: 19-32
- 14 Johann S, Heitzer M, Kanagaratnam M, Goswami A, Rizo T, Weis J, Troost D, Beyer C. NLRP3 inflammasome is expressed by astrocytes in the SOD1 mouse model of ALS and in human sporadic ALS patients. *Glia* 2015 Dec; **63**: 2260-73
- 15 Philips T, Robberecht W. Neuroinflammation in amyotrophic lateral sclerosis: role of glial activation in motor neuron disease. *The Lancet Neurology* 2011 Mar; **10**: 253-63
- 16 Martinon F. Signaling by ROS drives inflammasome activation. *European journal of immunology* 2010 Mar; **40**: 616-9
- 17 Schroder K, Tschopp J. The inflammasomes. *Cell* 2010 Mar 19; **140**: 821-32

- 18 Martinon F, Burns K, Tschopp J. The inflammasome: a molecular platform triggering activation of inflammatory caspases and processing of proIL-beta. *Molecular cell* 2002 Aug; **10**: 417-26
- 19 Sangiuliano B, Perez NM, Moreira DF, Belizario JE. Cell death-associated molecular-pattern molecules: inflammatory signaling and control. *Mediators of inflammation* 2014; **2014**: 821043
- 20 Denes A, Lopez-Castejon G, Brough D. Caspase-1: is IL-1 just the tip of the ICEberg? *Cell death & disease* 2012 Jul 05; **3**: e338
- 21 Dinarello CA. Interleukin-1 beta, interleukin-18, and the interleukin-1 beta converting enzyme. *Annals of the New York Academy of Sciences* 1998 Sep 29; **856**: 1-11
- 22 Barbe F, Douglas T, Saleh M. Advances in Nod-like receptors (NLR) biology. *Cytokine & growth factor reviews* 2014 Dec; **25**: 681-97
- 23 Poyet JL, Srinivasula SM, Tnani M, Razmara M, Fernandes-Alnemri T, Alnemri ES. Identification of Ipaf, a human caspase-1-activating protein related to Apaf-1. *The Journal of biological chemistry* 2001 Jul 27; **276**: 28309-13
- 24 Roberts TL, Idris A, Dunn JA, Kelly GM, Burnton CM, Hodgson S, Hardy LL, Garceau V, Sweet MJ, Ross IL, Hume DA, Stacey KJ. HIN-200 proteins regulate caspase activation in response to foreign cytoplasmic DNA. *Science (New York, NY)* 2009 Feb 20; **323**: 1057-60
- 25 Lamkanfi M, Dixit VM. Mechanisms and functions of inflammasomes. *Cell* 2014 May 22; **157**: 1013-22
- 26 Jin T, Curry J, Smith P, Jiang J, Xiao TS. Structure of the NLRP1 caspase recruitment domain suggests potential mechanisms for its association with procaspase-1. *Proteins* 2013 Jul; **81**: 1266-70
- 27 Chavarria-Smith J, Vance RE. The NLRP1 inflammasomes. *Immunological reviews* 2015 May; **265**: 22-34
- 28 Broz P, von Moltke J, Jones JW, Vance RE, Monack DM. Differential requirement for Caspase-1 autoproteolysis in pathogen-induced cell death and cytokine processing. *Cell host & microbe* 2010 Dec 16; **8**: 471-83
- 29 Heneka MT, Kummer MP, Stutz A, Delekate A, Schwartz S, Vieira-Saecker A, Griep A, Axt D, Remus A, Tzeng TC, Gelpi E, Halle A, Korte M, Latz E, Golenbock DT. NLRP3 is activated in Alzheimer's disease and contributes to pathology in APP/PS1 mice. *Nature* 2013 Jan 31; **493**: 674-8
- 30 Saresella M, La Rosa F, Piancone F, Zoppis M, Marventano I, Calabrese E, Rainone V, Nemni R, Mancuso R, Clerici M. The NLRP3 and NLRP1 inflammasomes are activated in Alzheimer's disease. *Molecular neurodegeneration* 2016 Mar 03; **11**: 23
- 31 Jha S, Srivastava SY, Brickey WJ, Iocca H, Toews A, Morrison JP, Chen VS, Gris D, Matsushima GK, Ting JP. The inflammasome sensor, NLRP3, regulates CNS inflammation and demyelination via caspase-1 and interleukin-18. *The Journal of neuroscience : the official journal of the Society for Neuroscience* 2010 Nov 24; **30**: 15811-20

- 32 Noroozi S, Meimand HA, Arababadi MK, Nakhaee N, Asadikaram G. The Effects of IFN-beta 1a on the Expression of Inflammasomes and Apoptosis-Associated Speck-Like Proteins in Multiple Sclerosis Patients. *Molecular neurobiology* 2016 Mar 31:
- 33 Fann DY, Lee SY, Manzanero S, Tang SC, Gelderblom M, Chunduri P, Bernreuther C, Glatzel M, Cheng YL, Thundyil J, Widiapradja A, Lok KZ, Foo SL, Wang YC, Li YI, Drummond GR, Basta M, Magnus T, Jo DG, Mattson MP, Sobey CG, Arumugam TV. Intravenous immunoglobulin suppresses NLRP1 and NLRP3 inflammasome-mediated neuronal death in ischemic stroke. *Cell death & disease* 2013 Sep 05; **4**: e790
- 34 Lammerding L, Slowik A, Johann S, Beyer C, Zendedel A. Poststroke Inflammasome Expression and Regulation in the Peri-Infarct Area by Gonadal Steroids after Transient Focal Ischemia in the Rat Brain. *Neuroendocrinology* 2016; **103**: 460-75
- 35 Yang F, Wang Z, Wei X, Han H, Meng X, Zhang Y, Shi W, Li F, Xin T, Pang Q, Yi F. NLRP3 deficiency ameliorates neurovascular damage in experimental ischemic stroke. *Journal of cerebral blood flow and metabolism : official journal of the International Society of Cerebral Blood Flow and Metabolism* 2014 Apr; **34**: 660-7
- 36 de Rivero Vaccari JP, Lotocki G, Marcillo AE, Dietrich WD, Keane RW. A molecular platform in neurons regulates inflammation after spinal cord injury. *The Journal of neuroscience : the official journal of the Society for Neuroscience* 2008 Mar 26; **28**: 3404-14
- 37 Zendedel A, Johann S, Mehrabi S, Joghataei MT, Hassanzadeh G, Kipp M, Beyer C. Activation and Regulation of NLRP3 Inflammasome by Intrathecal Application of SDF-1a in a Spinal Cord Injury Model. *Molecular neurobiology* 2016 Jul; **53**: 3063-75
- 38 Li M, Ona VO, Guegan C, Chen M, Jackson-Lewis V, Andrews LJ, Olszewski AJ, Stieg PE, Lee JP, Przedborski S, Friedlander RM. Functional role of caspase-1 and caspase-3 in an ALS transgenic mouse model. *Science (New York, NY)* 2000 Apr 14; **288**: 335-9
- 39 Meissner F, Molawi K, Zychlinsky A. Mutant superoxide dismutase 1-induced IL-1beta accelerates ALS pathogenesis. *Proceedings of the National Academy of Sciences of the United States of America* 2010 Jul 20; **107**: 13046-50
- 40 Vukosavic S, Stefanis L, Jackson-Lewis V, Guegan C, Romero N, Chen C, Dubois-Dauphin M, Przedborski S. Delaying caspase activation by Bcl-2: A clue to disease retardation in a transgenic mouse model of amyotrophic lateral sclerosis. *The Journal of neuroscience : the official journal of the Society for Neuroscience* 2000 Dec 15; **20**: 9119-25
- 41 Pasinelli P, Borchelt DR, Houseweart MK, Cleveland DW, Brown RH, Jr. Caspase-1 is activated in neural cells and tissue with amyotrophic lateral sclerosis-associated mutations in copper-zinc superoxide dismutase. *Proceedings of the National Academy of Sciences of the United States of America* 1998 Dec 22; **95**: 15763-8
- 42 Heitzer M, Kaiser S, Kanagaratnam M, Zendedel A, Hartmann P, Beyer C, Johann S. Administration of 17beta-Estradiol Improves Motoneuron Survival and Down-regulates Inflammasome Activation in Male SOD1(G93A) ALS Mice. 2016 Dec 12:

- 43 Pansarasa O, Rossi D, Berardinelli A, Cereda C. Amyotrophic lateral sclerosis and skeletal muscle: an update. *Molecular neurobiology* 2014 Apr; **49**: 984-90
- 44 Clement AM, Nguyen MD, Roberts EA, Garcia ML, Boillee S, Rule M, McMahon AP, Doucette W, Siwek D, Ferrante RJ, Brown RH, Jr., Julien JP, Goldstein LS, Cleveland DW. Wild-type nonneuronal cells extend survival of SOD1 mutant motor neurons in ALS mice. *Science (New York, NY)* 2003 Oct 03; **302**: 113-7
- 45 Nagai M, Re DB, Nagata T, Chalazonitis A, Jessell TM, Wichterle H, Przedborski S. Astrocytes expressing ALS-linked mutated SOD1 release factors selectively toxic to motor neurons. *Nature neuroscience* 2007 May; **10**: 615-22
- 46 Haidet-Phillips AM, Hester ME, Miranda CJ, Meyer K, Braun L, Frakes A, Song S, Likhite S, Murtha MJ, Foust KD, Rao M, Eagle A, Kammesheidt A, Christensen A, Mendell JR, Burghes AH, Kaspar BK. Astrocytes from familial and sporadic ALS patients are toxic to motor neurons. *Nature biotechnology* 2011 Aug 10; **29**: 824-8
- 47 Wong M, Martin LJ. Skeletal muscle-restricted expression of human SOD1 causes motor neuron degeneration in transgenic mice. *Human molecular genetics* 2010 Jun 01; **19**: 2284-302
- 48 Dupuis L, di Scala F, Rene F, de Tapia M, Oudart H, Pradat PF, Meininger V, Loeffler JP. Up-regulation of mitochondrial uncoupling protein 3 reveals an early muscular metabolic defect in amyotrophic lateral sclerosis. *FASEB journal : official publication of the Federation of American Societies for Experimental Biology* 2003 Nov; **17**: 2091-3
- 49 Luo G, Yi J, Ma C, Xiao Y, Yi F, Yu T, Zhou J. Defective mitochondrial dynamics is an early event in skeletal muscle of an amyotrophic lateral sclerosis mouse model. *PLoS one* 2013; **8**: e82112
- 50 Olivan S, Calvo AC, Gasco S, Munoz MJ, Zaragoza P, Osta R. Time-Point Dependent Activation of Autophagy and the UPS in SOD1G93A Mice Skeletal Muscle. *PLoS one* 2015; **10**: e0134830
- 51 Dobrowolny G, Aucello M, Rizzuto E, Beccafico S, Mammucari C, Boncompagni S, Belia S, Wannenes F, Nicoletti C, Del Prete Z, Rosenthal N, Molinaro M, Protasi F, Fano G, Sandri M, Musaro A. Skeletal muscle is a primary target of SOD1G93A-mediated toxicity. *Cell metabolism* 2008 Nov; **8**: 425-36
- 52 de Oliveira GP, Maximino JR, Maschietto M, Zanoteli E, Puga RD, Lima L, Carraro DM, Chadi G. Early gene expression changes in skeletal muscle from SOD1(G93A) amyotrophic lateral sclerosis animal model. *Cellular and molecular neurobiology* 2014 Apr; **34**: 451-62
- 53 Galbiati M, Onesto E, Zito A, Crippa V, Rusmini P, Mariotti R, Bentivoglio M, Bendotti C, Poletti A. The anabolic/androgenic steroid nandrolone exacerbates gene expression modifications induced by mutant SOD1 in muscles of mice models of amyotrophic lateral sclerosis. *Pharmacological research* 2012 Feb; **65**: 221-30
- 54 Jesse CM, Bushuven E, Tripathi P, Chandrasekar A, Simon CM, Drepper C, Yamoah A, Dreser A, Katona I, Johann S, Beyer C, Wagner S, Grond M, Nikolin S, Anink J, Troost D, Sendtner M, Goswami A, Weis J. ALS-Associated Endoplasmic Reticulum Proteins in Denervated Skeletal Muscle: Implications for Motor Neuron Disease Pathology. *Brain pathology (Zurich, Switzerland)* 2016 Oct 28:

- 55 Jensen L, Jorgensen LH, Bech RD, Frandsen U, Schroder HD. Skeletal Muscle Remodelling as a Function of Disease Progression in Amyotrophic Lateral Sclerosis. *BioMed research international* 2016; **2016**: 5930621
- 56 Van Dyke JM, Smit-Oistad IM, Macrander C, Krakora D, Meyer MG, Suzuki M. Macrophage-mediated inflammation and glial response in the skeletal muscle of a rat model of familial amyotrophic lateral sclerosis (ALS). *Experimental neurology* 2016 Mar; **277**: 275-82
- 57 Scott S, Kranz JE, Cole J, Lincecum JM, Thompson K, Kelly N, Bostrom A, Theodoss J, Al-Nakhala BM, Vieira FG, Ramasubbu J, Heywood JA. Design, power, and interpretation of studies in the standard murine model of ALS. *Amyotrophic lateral sclerosis : official publication of the World Federation of Neurology Research Group on Motor Neuron Diseases* 2008; **9**: 4-15
- 58 Alexander GM, Erwin KL, Byers N, Deitch JS, Augelli BJ, Blankenhorn EP, Heiman-Patterson TD. Effect of transgene copy number on survival in the G93A SOD1 transgenic mouse model of ALS. *Brain research Molecular brain research* 2004 Nov 4; **130**: 7-15
- 59 Walsh JG, Muruve DA, Power C. Inflammasomes in the CNS. *Nature reviews Neuroscience* 2014 Feb; **15**: 84-97
- 60 Singhal G, Jaehne EJ, Corrigan F, Toben C, Baune BT. Inflammasomes in neuroinflammation and changes in brain function: a focused review. *Frontiers in neuroscience* 2014; **8**: 315
- 61 de Rivero Vaccari JP, Dietrich WD, Keane RW. Activation and regulation of cellular inflammasomes: gaps in our knowledge for central nervous system injury. *Journal of cerebral blood flow and metabolism : official journal of the International Society of Cerebral Blood Flow and Metabolism* 2014 Mar; **34**: 369-75
- 62 Ye X, Shen T, Hu J, Zhang L, Zhang Y, Bao L, Cui C, Jin G, Zan K, Zhang Z, Yang X, Shi H, Zu J, Yu M, Song C, Wang Y, Qi S, Cui G. Purinergic 2X7 receptor/NLRP3 pathway triggers neuronal apoptosis after ischemic stroke in the mouse. *Experimental neurology* 2017 Jun; **292**: 46-55
- 63 Coll RC, Robertson AA, Chae JJ, Higgins SC, Munoz-Planillo R, Inserra MC, Vetter I, Dungan LS, Monks BG, Stutz A, Croker DE, Butler MS, Haneklaus M, Sutton CE, Nunez G, Latz E, Kastner DL, Mills KH, Masters SL, Schroder K, Cooper MA, O'Neill LA. A small-molecule inhibitor of the NLRP3 inflammasome for the treatment of inflammatory diseases. *Nature medicine* 2015 Mar; **21**: 248-55
- 64 Dempsey C, Rubio Araiz A, Bryson KJ, Finucane O, Larkin C, Mills EL, Robertson AAB, Cooper MA, O'Neill LAJ, Lynch MA. Inhibiting the NLRP3 inflammasome with MCC950 promotes non-phlogistic clearance of amyloid-beta and cognitive function in APP/PS1 mice. *Brain, behavior, and immunity* 2017 Mar; **61**: 306-16
- 65 Boyer JG, Ferrier A, Kothary R. More than a bystander: the contributions of intrinsic skeletal muscle defects in motor neuron diseases. *Frontiers in physiology* 2013 Dec 18; **4**: 356
- 66 Moloney EB, de Winter F, Verhaagen J. ALS as a distal axonopathy: molecular mechanisms affecting neuromuscular junction stability in the presymptomatic stages of the disease. *Frontiers in neuroscience* 2014; **8**: 252

- 67 Dupuis L, Gonzalez de Aguilar JL, Echaniz-Laguna A, Eschbach J, Rene F, Oudart H, Halter B, Huze C, Schaeffer L, Bouillaud F, Loeffler JP. Muscle mitochondrial uncoupling dismantles neuromuscular junction and triggers distal degeneration of motor neurons. *PloS one* 2009; **4**: e5390
- 68 Hegedus J, Putman CT, Gordon T. Time course of preferential motor unit loss in the SOD1 G93A mouse model of amyotrophic lateral sclerosis. *Neurobiology of disease* 2007 Nov; **28**: 154-64
- 69 Rocha MC, Pousinha PA, Correia AM, Sebastiao AM, Ribeiro JA. Early changes of neuromuscular transmission in the SOD1(G93A) mice model of ALS start long before motor symptoms onset. *PloS one* 2013; **8**: e73846
- 70 Gonzalez de Aguilar JL, Niederhauser-Wiederkehr C, Halter B, De Tapia M, Di Scala F, Demougin P, Dupuis L, Primig M, Meininger V, Loeffler JP. Gene profiling of skeletal muscle in an amyotrophic lateral sclerosis mouse model. *Physiological genomics* 2008 Jan 17; **32**: 207-18
- 71 Thau N, Knippenberg S, Korner S, Rath KJ, Dengler R, Petri S. Decreased mRNA expression of PGC-1alpha and PGC-1alpha-regulated factors in the SOD1G93A ALS mouse model and in human sporadic ALS. *Journal of neuropathology and experimental neurology* 2012 Dec; **71**: 1064-74
- 72 Frost RA, Lang CH. Regulation of muscle growth by pathogen-associated molecules. *Journal of animal science* 2008 Apr; **86**: E84-93
- 73 Nishimura M, Naito S. Tissue-specific mRNA expression profiles of human toll-like receptors and related genes. *Biological & pharmaceutical bulletin* 2005 May; **28**: 886-92
- 74 Pillon NJ, Krook A. Innate immune receptors in skeletal muscle metabolism. *Experimental cell research* 2017 Feb 21:
- 75 Marino M, Scuderi F, Provenzano C, Bartoccioni E. Skeletal muscle cells: from local inflammatory response to active immunity. *Gene therapy* 2011 Feb; **18**: 109-16
- 76 Friedlander RM, Brown RH, Gagliardini V, Wang J, Yuan J. Inhibition of ICE slows ALS in mice. *Nature* 1997 Jul 03; **388**: 31
- 77 De Rossi M, Bernasconi P, Baggi F, de Waal Malefyt R, Mantegazza R. Cytokines and chemokines are both expressed by human myoblasts: possible relevance for the immune pathogenesis of muscle inflammation. *International immunology* 2000 Sep; **12**: 1329-35
- 78 Cohen TV, Many GM, Fleming BD, Gnocchi VF, Ghimbovschi S, Mosser DM, Hoffman EP, Partridge TA. Upregulated IL-1beta in dysferlin-deficient muscle attenuates regeneration by blunting the response to pro-inflammatory macrophages. *Skeletal muscle* 2015; **5**: 24
- 79 Tucci M, Quatraro C, Dammacco F, Silvestris F. Interleukin-18 overexpression as a hallmark of the activity of autoimmune inflammatory myopathies. *Clinical and experimental immunology* 2006 Oct; **146**: 21-31
- 80 Schmidt J, Barthel K, Wrede A, Salajegheh M, Bahr M, Dalakas MC. Interrelation of inflammation and APP in sIBM: IL-1 beta induces accumulation of beta-amyloid in skeletal muscle. *Brain : a journal of neurology* 2008 May; **131**: 1228-40

- 81 Rawat R, Cohen TV, Ampong B, Francia D, Henriques-Pons A, Hoffman EP, Nagaraju K. Inflammasome up-regulation and activation in dysferlin-deficient skeletal muscle. *The American journal of pathology* 2010 Jun; **176**: 2891-900
- 82 Dobrowolny G, Aucello M, Musaro A. Muscle atrophy induced by SOD1G93A expression does not involve the activation of caspase in the absence of denervation. *Skeletal muscle* 2011 Jan 24; **1**: 3
- 83 Puren AJ, Fantuzzi G, Dinarello CA. Gene expression, synthesis, and secretion of interleukin 18 and interleukin 1beta are differentially regulated in human blood mononuclear cells and mouse spleen cells. *Proceedings of the National Academy of Sciences of the United States of America* 1999 Mar 2; **96**: 2256-61
- 84 Netea MG, Joosten LA, Lewis E, Jensen DR, Voshol PJ, Kullberg BJ, Tack CJ, van Krieken H, Kim SH, Stalenoef AF, van de Loo FA, Verschueren I, Pulawa L, Akira S, Eckel RH, Dinarello CA, van den Berg W, van der Meer JW. Deficiency of interleukin-18 in mice leads to hyperphagia, obesity and insulin resistance. *Nature medicine* 2006 Jun; **12**: 650-6
- 85 Lindegaard B, Hvid T, Wolsk Mygind H, Hartvig-Mortensen O, Grondal T, Abildgaard J, Gerstoft J, Pedersen BK, Baranowski M. Low expression of IL-18 and IL-18 receptor in human skeletal muscle is associated with systemic and intramuscular lipid metabolism-Role of HIV lipodystrophy. *PLoS one* 2018; **13**: e0186755
- 86 Lindegaard B, Matthews VB, Brandt C, Hojman P, Allen TL, Estevez E, Watt MJ, Bruce CR, Mortensen OH, Syberg S, Rudnicka C, Abildgaard J, Pilegaard H, Hidalgo J, Ditlevsen S, Alsted TJ, Madsen AN, Pedersen BK, Febbraio MA. Interleukin-18 activates skeletal muscle AMPK and reduces weight gain and insulin resistance in mice. *Diabetes* 2013 Sep; **62**: 3064-74
- 87 Hazuda DJ, Lee JC, Young PR. The kinetics of interleukin 1 secretion from activated monocytes. Differences between interleukin 1 alpha and interleukin 1 beta. *The Journal of biological chemistry* 1988 Jun 15; **263**: 8473-9
- 88 McBride MJ, Foley KP, D'Souza D M, Li YE, Lau TC, Hawke TJ, Schertzer JD. The NLRP3 inflammasome contributes to sarcopenia and lower muscle glycolytic potential in old mice. *American journal of physiology Endocrinology and metabolism* 2017 May 23: ajpendo 00060 2017
- 89 Kien CL, Bunn JY, Fukagawa NK, Anathy V, Matthews DE, Crain KI, Ebenstein DB, Tarleton EK, Pratley RE, Poynter ME. Lipidomic evidence that lowering the typical dietary palmitate to oleate ratio in humans decreases the leukocyte production of proinflammatory cytokines and muscle expression of redox-sensitive genes. *The Journal of nutritional biochemistry* 2015 Dec; **26**: 1599-606
- 90 Huang N, Kny M, Riediger F, Busch K, Schmidt S, Luft FC, Slevogt H, Fielitz J. Deletion of Nlrp3 protects from inflammation-induced skeletal muscle atrophy. *Intensive care medicine experimental* 2017 Dec; **5**: 3
- 91 Hornung V, Ablasser A, Charrel-Dennis M, Bauernfeind F, Horvath G, Caffrey DR, Latz E, Fitzgerald KA. AIM2 recognizes cytosolic dsDNA and forms a caspase-1-activating inflammasome with ASC. *Nature* 2009 Mar 26; **458**: 514-8

- 92 Fernandes-Alnemri T, Yu JW, Datta P, Wu J, Alnemri ES. AIM2 activates the inflammasome and cell death in response to cytoplasmic DNA. *Nature* 2009 Mar 26; **458**: 509-13
- 93 Burckstummer T, Baumann C, Bluml S, Dixit E, Durnberger G, Jahn H, Planyavsky M, Bilban M, Colinge J, Bennett KL, Superti-Furga G. An orthogonal proteomic-genomic screen identifies AIM2 as a cytoplasmic DNA sensor for the inflammasome. *Nature immunology* 2009 Mar; **10**: 266-72
- 94 Liu T, Tang Q, Liu K, Xie W, Liu X, Wang H, Wang RF, Cui J. TRIM11 Suppresses AIM2 Inflammasome by Degrading AIM2 via p62-Dependent Selective Autophagy. *Cell reports* 2016 Aug 16; **16**: 1988-2002
- 95 Shi CS, Shenderov K, Huang NN, Kabat J, Abu-Asab M, Fitzgerald KA, Sher A, Kehrl JH. Activation of autophagy by inflammatory signals limits IL-1beta production by targeting ubiquitinated inflammasomes for destruction. *Nature immunology* 2012 Jan 29; **13**: 255-63
- 96 Hu B, Jin C, Li HB, Tong J, Ouyang X, Cetinbas NM, Zhu S, Strowig T, Lam FC, Zhao C, Henao-Mejia J, Yilmaz O, Fitzgerald KA, Eisenbarth SC, Elinav E, Flavell RA. The DNA-sensing AIM2 inflammasome controls radiation-induced cell death and tissue injury. *Science (New York, NY)* 2016 Nov 11; **354**: 765-8
- 97 *Molecular neurobiology*:
- 98 Sastalla I, Crown D, Masters SL, McKenzie A, Leppla SH, Moayeri M. Transcriptional analysis of the three Nlrp1 paralogs in mice. *BMC genomics* 2013 Mar 18; **14**: 188
- 99 Chavarria-Smith J, Mitchell PS, Ho AM. Functional and Evolutionary Analyses Identify Proteolysis as a General Mechanism for NLRP1 Inflammasome Activation. 2016 Dec; **12**: e1006052
- 100 Masters SL, Gerlic M, Metcalf D, Preston S, Pellegrini M, O'Donnell JA, McArthur K, Baldwin TM, Chevrier S, Nowell CJ, Cengia LH, Henley KJ, Collinge JE, Kastner DL, Feigenbaum L, Hilton DJ, Alexander WS, Kile BT, Croker BA. NLRP1 inflammasome activation induces pyroptosis of hematopoietic progenitor cells. *Immunity* 2012 Dec 14; **37**: 1009-23
- 101 Faustin B, Lartigue L, Bruey JM, Luciano F, Sergienko E, Bailly-Maitre B, Volkmann N, Hanein D, Rouiller I, Reed JC. Reconstituted NALP1 inflammasome reveals two-step mechanism of caspase-1 activation. *Molecular cell* 2007 Mar 09; **25**: 713-24
- 102 Faustin B, Chen Y, Zhai D, Le Negrate G, Lartigue L, Satterthwait A, Reed JC. Mechanism of Bcl-2 and Bcl-X(L) inhibition of NLRP1 inflammasome: loop domain-dependent suppression of ATP binding and oligomerization. *Proceedings of the National Academy of Sciences of the United States of America* 2009 Mar 10; **106**: 3935-40
- 103 Liao KC, Mogridge J. Activation of the Nlrp1b inflammasome by reduction of cytosolic ATP. *Infection and immunity* 2013 Feb; **81**: 570-9
- 104 Frew BC, Joag VR, Mogridge J. Proteolytic processing of Nlrp1b is required for inflammasome activity. *PLoS pathogens* 2012; **8**: e1002659

- 105 Finger JN, Lich JD, Dare LC, Cook MN, Brown KK, Duraiswami C, Bertin J, Gough PJ. Autolytic proteolysis within the function to find domain (FIIND) is required for NLRP1 inflammasome activity. *The Journal of biological chemistry* 2012 Jul 20; **287**: 25030-7
- 106 Baker PJ, De Nardo D, Moghaddas F, Tran LS, Bachem A, Nguyen T, Hayman T, Tye H, Vince JE, Bedoui S, Ferrero RL, Masters SL. Posttranslational Modification as a Critical Determinant of Cytoplasmic Innate Immune Recognition. *Physiological reviews* 2017 Jul 1; **97**: 1165-209
- 107 D'Oswaldo A, Weichenberger CX, Wagner RN, Godzik A, Wooley J, Reed JC. CARD8 and NLRP1 undergo autoproteolytic processing through a ZU5-like domain. *PLoS one* 2011; **6**: e27396
- 108 Hellmich KA, Levinsohn JL, Fattah R, Newman ZL, Maier N, Sastalla I, Liu S, Leppla SH, Moayeri M. Anthrax lethal factor cleaves mouse nlrp1b in both toxin-sensitive and toxin-resistant macrophages. *PLoS one* 2012; **7**: e49741
- 109 Levinsohn JL, Newman ZL, Hellmich KA, Fattah R, Getz MA, Liu S, Sastalla I, Leppla SH, Moayeri M. Anthrax lethal factor cleavage of Nlrp1 is required for activation of the inflammasome. *PLoS pathogens* 2012; **8**: e1002638
- 110 Goodman CA, Kotecki JA, Jacobs BL, Hornberger TA. Muscle fiber type-dependent differences in the regulation of protein synthesis. *PLoS one* 2012; **7**: e37890
- 111 Franchi L, Amer A, Body-Malapel M, Kanneganti TD, Ozoren N, Jagirdar R, Inohara N, Vandenabeele P, Bertin J, Coyle A, Grant EP, Nunez G. Cytosolic flagellin requires Ipaf for activation of caspase-1 and interleukin 1beta in salmonella-infected macrophages. *Nature immunology* 2006 Jun; **7**: 576-82
- 112 Miao EA, Alpuche-Aranda CM, Dors M, Clark AE, Bader MW, Miller SI, Aderem A. Cytoplasmic flagellin activates caspase-1 and secretion of interleukin 1beta via Ipaf. *Nature immunology* 2006 Jun; **7**: 569-75
- 113 Freeman L, Guo H, David CN, Brickey WJ, Jha S, Ting JP. NLR members NLRC4 and NLRP3 mediate sterile inflammasome activation in microglia and astrocytes. *The Journal of experimental medicine* 2017 May 01; **214**: 1351-70
- 114 Denes A, Coutts G, Lenart N, Cruickshank SM, Pelegrin P, Skinner J, Rothwell N, Allan SM, Brough D. AIM2 and NLRC4 inflammasomes contribute with ASC to acute brain injury independently of NLRP3. *Proceedings of the National Academy of Sciences of the United States of America* 2015 Mar 31; **112**: 4050-5
- 115 DeSantis DA, Ko CW, Liu Y, Liu X, Hise AG, Nunez G, Croniger CM. Alcohol-induced liver injury is modulated by Nlrp3 and Nlrc4 inflammasomes in mice. *Mediators of inflammation* 2013; **2013**: 751374
- 116 Damiano JS, Stehlik C, Pio F, Godzik A, Reed JC. CLAN, a novel human CED-4-like gene. *Genomics* 2001 Jul; **75**: 77-83

- 117 Schieber AM, Lee YM, Chang MW, Leblanc M, Collins B, Downes M, Evans RM, Ayres JS. Disease tolerance mediated by microbiome *E. coli* involves inflammasome and IGF-1 signaling. *Science (New York, NY)* 2015 Oct 30; **350**: 558-63
- 118 Karan D, Tawfik O, Dubey S. Expression analysis of inflammasome sensors and implication of NLRP12 inflammasome in prostate cancer. *Scientific reports* 2017 Jun 29; **7**: 4378
- 119 Franchi L, Warner N, Viani K, Nunez G. Function of Nod-like receptors in microbial recognition and host defense. *Immunological reviews* 2009 Jan; **227**: 106-28
- 120 Wang HA, Lee JD, Lee KM, Woodruff TM, Noakes PG. Complement C5a-C5aR1 signalling drives skeletal muscle macrophage recruitment in the hSOD1G93A mouse model of amyotrophic lateral sclerosis. *Skeletal muscle* 2017 Jun 01; **7**: 10
- 121 Chiu IM, Phatnani H, Kuligowski M, Tapia JC, Carrasco MA, Zhang M, Maniatis T, Carroll MC. Activation of innate and humoral immunity in the peripheral nervous system of ALS transgenic mice. *Proceedings of the National Academy of Sciences of the United States of America* 2009 Dec 08; **106**: 20960-5
- 122 Troost D, Das PK, van den Oord JJ, Louwse ES. Immunohistological alterations in muscle of patients with amyotrophic lateral sclerosis: mononuclear cell phenotypes and expression of MHC products. *Clinical neuropathology* 1992 May-Jun; **11**: 115-20
- 123 Al-Sarraj S, King A, Cleveland M, Pradat PF, Corse A, Rothstein JD, Leigh PN, Abila B, Bates S, Wurthner J, Meininger V. Mitochondrial abnormalities and low grade inflammation are present in the skeletal muscle of a minority of patients with amyotrophic lateral sclerosis; an observational myopathology study. *Acta neuropathologica communications* 2014 Dec 14; **2**: 165
- 124 Yang J, Liu Z, Xiao TS. Post-translational regulation of inflammasomes. *Cellular & molecular immunology* 2017 Jan; **14**: 65-79
- 125 He Y, Hara H, Nunez G. Mechanism and Regulation of NLRP3 Inflammasome Activation. *Trends in biochemical sciences* 2016 Dec; **41**: 1012-21
- 126 Dinarello CA. Interleukin-1, interleukin-1 receptors and interleukin-1 receptor antagonist. *International reviews of immunology* 1998; **16**: 457-99
- 127 Fenton MJ. Review: transcriptional and post-transcriptional regulation of interleukin 1 gene expression. *International journal of immunopharmacology* 1992 Apr; **14**: 401-11
- 128 Turner M, Chantry D, Feldmann M. Post-transcriptional control of IL-1 gene expression in the acute monocytic leukemia line THP-1. *Biochemical and biophysical research communications* 1988 Oct 31; **156**: 830-9

Figure legends

Figure 1 Histopathology of skeletal muscle from SOD1^(G93A) mice and human patients

(**A-F**) Representative H&E staining of skeletal muscle tissue from SOD1^(G93A) mice (**A-C**) and human control and sALS patients (**D-F**). No obvious abnormalities in muscle morphology were observed in WT (**A**) and 9W old SOD1 mice (**B**), as well as in the human control subject (**D**). However, in 14W old SOD1 animals (**C**) and in sALS patients (**E-F**), typical features of neurogenic atrophy, including muscle fibre atrophy (**C, E-F**; inset, black arrow), compensatory hypertrophy (**C, E**; inset, arrowhead) and central myonuclei were detected (**C, E**; asterisk).

Figure 2 Increased protein levels of aCasp 1 and IL1 β in SOD1^(G93A) mice and human patients

(**A-Q**) Western Blot analysis was performed using antibodies against caspase 1, IL1 β and IL18. Pro-Casp1 (30-46 kDa) and pro-IL1 β (32 kDa) were expressed in 9W (**A**) and 14W (**B**) old WT and SOD1 mice. Pro-Casp1 (* $p=0.0407$), but not pro-IL1 β was significantly upregulated in 14W old SOD1 animals (**C-J**). Active caspase 1 (p20) and mature IL1 β (17 kDa) were significantly increased in 9W (** $p=0.0022$ and * $p=0.0103$, respectively) and 14W (* $p=0.0159$ and * $p=0.0159$, respectively) old SOD1 mice (**C-J**). Pro- and mature IL18 were not significantly altered in SOD1 mice (**K-N**). Although the active peptides were not detected in human samples, a significant increase of pro-casp1 (intermediate p35-kDa fragment) and pro-IL1 β was noticed in sALS (**O, P-Q**; ** $p=0.0095$ and ** $p=0.0089$, respectively). Data represent means \pm SEM from $n=4-5$. Student's t-test: * $p<0.05$ and ** $p<0.01$ vs. WT/Control or Mann-Whitney U test (mature IL1 β): * $p<0.05$ vs WT/Control.

Figure 3 Expression of PRRs in 9W old WT and pre-symptomatic SOD1^(G93A) mice

(**A-H**) Western Blot data of PRRs and ASC in the skeletal muscle from pre-symptomatic SOD1 animals. Two products of NLRP1, the canonical isoform with 165 kDa and a smaller 15-kDa fragment were expressed, but not significantly altered in SOD1 mice (**A-C**). Only the 18- and 40-kDa products, but not the canonical 116-kDa isoform of NLRC4 were detected by Western Blot in WT and SOD1 animals (**A, D-**

E). However, protein levels of the 18-kDa product were significantly increased (E; $**p=0.0040$). Expression of NLRP3 and AIM2 were not significantly different (A, F-G), Instead of the expected 22-kDa ASC monomer, an immunoreactive band of approx. 35 kDa was detected (H). Data represent means \pm SEM from $n=4-5$. Student's t-test: $**p<0.01$ vs. WT.

Figure 4 Expression of PRRs in 14W old WT and symptomatic SOD1^(G93A) mice

(A-I) Western Blot data of PRRs and ASC in the skeletal muscle from symptomatic SOD1 animals. The 165-kDa isoform and the 15-kDa fragment of NLRP1 were expressed in WT and SOD1 animals (A-C). A significant down-regulation of the canonical NLRP1 was detected in SOD1 mice (B, $*p=0.0351$). The 116-kDa canonical, and the two smaller products of NLRC4 were significantly increased in both genotypes (A, D-F $*p=0.0469$, $**p=0.0045$ and $**p=0.0015$, respectively). Expression levels of AIM2 (A, H; $*p=0.0118$) but not NLRP3 (A, G) were significantly increased in SOD1 animals. Expression levels of the 22- and 35-kDa ASC product were not significantly different (A, I). Data represent means \pm SEM from $n=4-5$. Student's t-test: $*p<0.05$, $**p<0.01$ vs. WT.

Figure 5 Transcription levels of PRRs, ASC and interleukins in WT and SOD1^(G93A) mice

(A-G) Realtime PCR analysis of inflammasome components in skeletal muscle of 9W and 14W old WT and SOD1 mice. A significant interaction was observed for NLRC4 (B; age*genotype $p=0.0180$, $F=6.44$, $Df=24$). Pairwise comparison revealed significant reduction of NLRC4 mRNA in 9W ($*p=0.0398$) but not 14W old SOD1 mice. No differences in mRNA expression were detected for the remaining PRRs (A, C-D). Two-way ANOVA indicated that genotype significantly effects the overall ASC ($p=0.0007$; $F=15.36$, $Df=23$) and IL18 ($p=0.0005$; $F=16.11$, $Df=23$) expression independent of age. However, a significant reduction of mRNA was observed for ASC (E, $**p=0.0021$) and for IL18 (F, $***p=0.0006$) in 14W old SOD1 animals. No changes in IL1 β mRNA levels were detected (G). Data represent means \pm SEM from $n=6-7$. $*p<0.05$ $**p<0.01$ and $***p<0.001$ by Bonferroni post-hoc tests following two-way ANOVA.

Figure 6 Tissue expression of PRRs in WT SOD1^(G93A) mice

(A-T) Representative immunohistochemistry of NLRP1, NLRC4, NLRP3, AIM2 and ASC from WT and SOD1 mice. (A-C) Intermyoibrillar staining of NLRP1 was detected in WT (A) and SOD1 mice (B-C). Some fibres were intensively and other weakly stained for NLRP1 (A-C; inset, asterisk). No significant differences in the immunoreactive area were detected (D). NLRC4 was localized in the intermyofibrillar (E-G; inset, asterisks) and subsarcolemmal compartment (G; inset, white arrowhead). Additionally, NLRC4 immunoreactivity was detected near the nuclear rim of 9 and 14W old SOD1 mice (F-G; inset, black arrowheads). A significant interaction was observed for NLRC4 (H; age*genotype $p=0.0051$, $F=11.69$, $Df=12$). Pairwise comparison revealed significant increase of NLRC4 immunoreactivity in 14W old SOD1 mice (** $p=0.0066$). The NLRP3 signal was weak and mainly localized to the nuclear rim in WT (I) and SOD1 animals (J-K; inset, arrowheads). Furthermore, other cells than muscle fibres, most likely macrophages, were NLRP3 positive (K; inset, arrow). No significant difference in the immunoreactive area was detected (L). Expression of AIM2 was localized to myonuclei (M-O; inset, arrowheads) and the interfibrillar compartment (M-O; inset, asterisks). Immunoreactivity of AIM2 was not significantly different in SOD1 mice (P). Although the overall signal of ASC was weak (Q-S), a subsarcolemmal (Q-S; inset, white arrowheads) and intermyofibrillar staining was detected (M-O; inset, asterisks). Single muscle fibres in 14W old SOD1 mice displayed strong ASC immunoreactivity (O). However, the immunoreactive area was similar in WT and SOD1 animals (T). Data represent means \pm SEM from $n=4$. Two-way ANOVA followed by Bonferroni's post hoc analysis: ** $p<0.01$ vs. WT.

Figure 7 Increased expression levels of PRRs in the skeletal muscle of sALS patients

(A-G) Western Blot data of different PRRs and ASC in the skeletal muscle from control (C) and sALS patients. Expression of the canonical isoform of NLRP1 (165 kDa) and the 15-kDa fragment was not significantly different in sALS patients (A-C). The canonical 116-kDa and the smaller 40- and 18-kDa products of NLRC4 were detected, but only levels of the 18-kDa isoform were significantly increased in sALS patients. (A, D-E; * $p=0.0307$). AIM2 expression was not significantly altered in sALS (A, F). A 35-kDa product, but not the 22-kDa ASC monomer was expressed at similar

levels in control and sALS subjects. (**A, G**). No detectable signal was found for NLRP3 and IL18 (**A**). Data represent means \pm SEM from n=3-5. Student's t-test: *p<0.05, **p<0.01 vs. Control.

Figure 8 Subcellular localization of PRRs in human patients

(**A-T**) Representative Immunohistochemistry of NLRP1, NLRC4, NLRP3, AIM2 and ASC in muscle biopsies from control and sALS patients. NLRP1 was localized in the intermyofibrillar compartment and isolated muscle fibres exhibit a stronger signal than others (**A-C**; inset, asterisks). No significant differences in the immunoreactive area were detected (**D**). NLRC4 immunoreactivity was detected in the nucleoplasm (**E-G**, inset, black arrowheads) and to a lesser extent in intermyofibrillar compartment (**F-G**, inset, asterisks). NLRC4 negative nuclei were detected in control muscle fibres (**E**; inset, black arrowhead), whereas myonuclei from atrophic fibres were NLRC4 positive (**F-G**; inset, black arrowheads). NLRC4 immunoreactivity was significantly increased in sALS patients (**H**, *p=0.0231). A faint cytoplasmic (**I-K**; inset, asterisks) and nuclear (**J-K**; inset, black arrowhead) immunoreactivity for NLRP3 was seen in control and sALS. Isolated cells between muscle fibres were also found NLRP3 positive (**J**; inset, arrow). NLRP3 immunoreactivity was similar in control and sALS patients (**L**). AIM2 (**M-O**) and ASC (**Q-S**) were expressed in the intermyofibrillar compartment (**M-S**; inset, asterisks) and single myonuclei were positive for AIM2 (**N-O**; inset, black arrowhead). Furthermore, cells located between muscle fibres of control and sALS were found positive for AIM2 (**N**; inset, arrow) and ASC (**Q-S**; inset, arrow). These cells most likely represent macrophages. Immunoreactivity of AIM2 (**P**) and ASC (**T**) was not significantly altered in sALS patients. Data represent means \pm SEM from n=3-5. Student's t-test: **p<0.01 vs. Control.

Figure 1

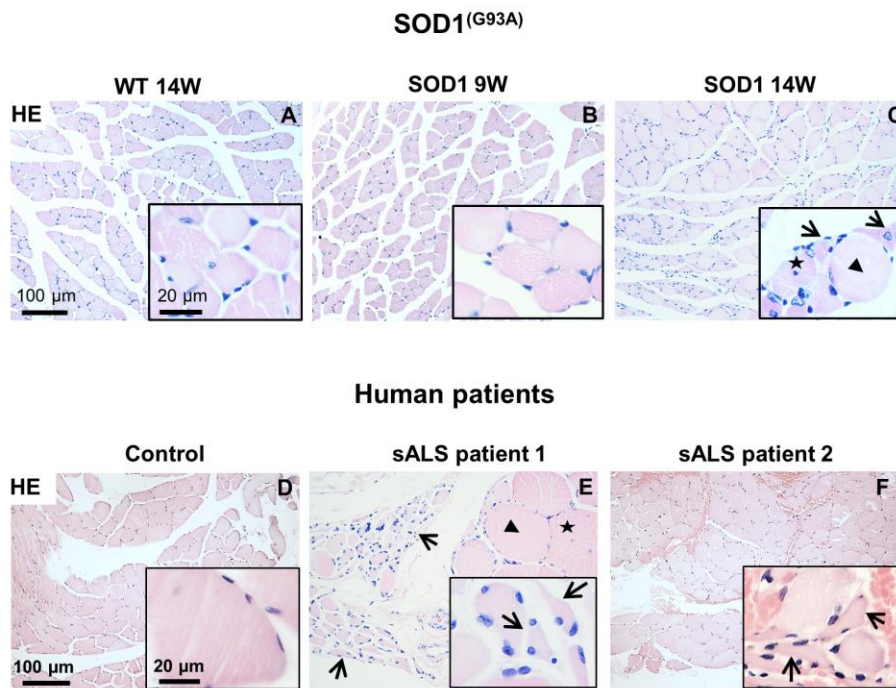


Figure 2

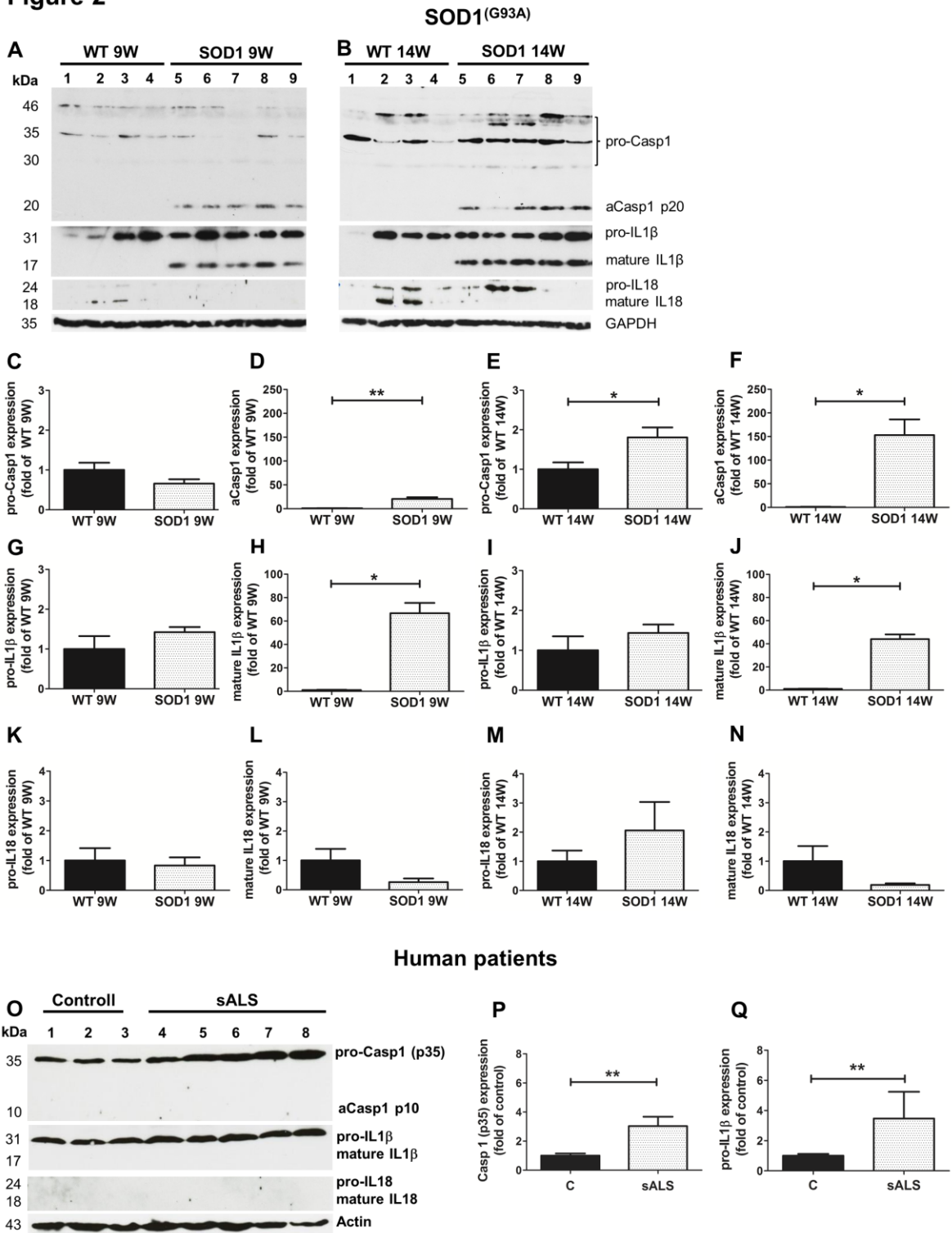


Figure 3

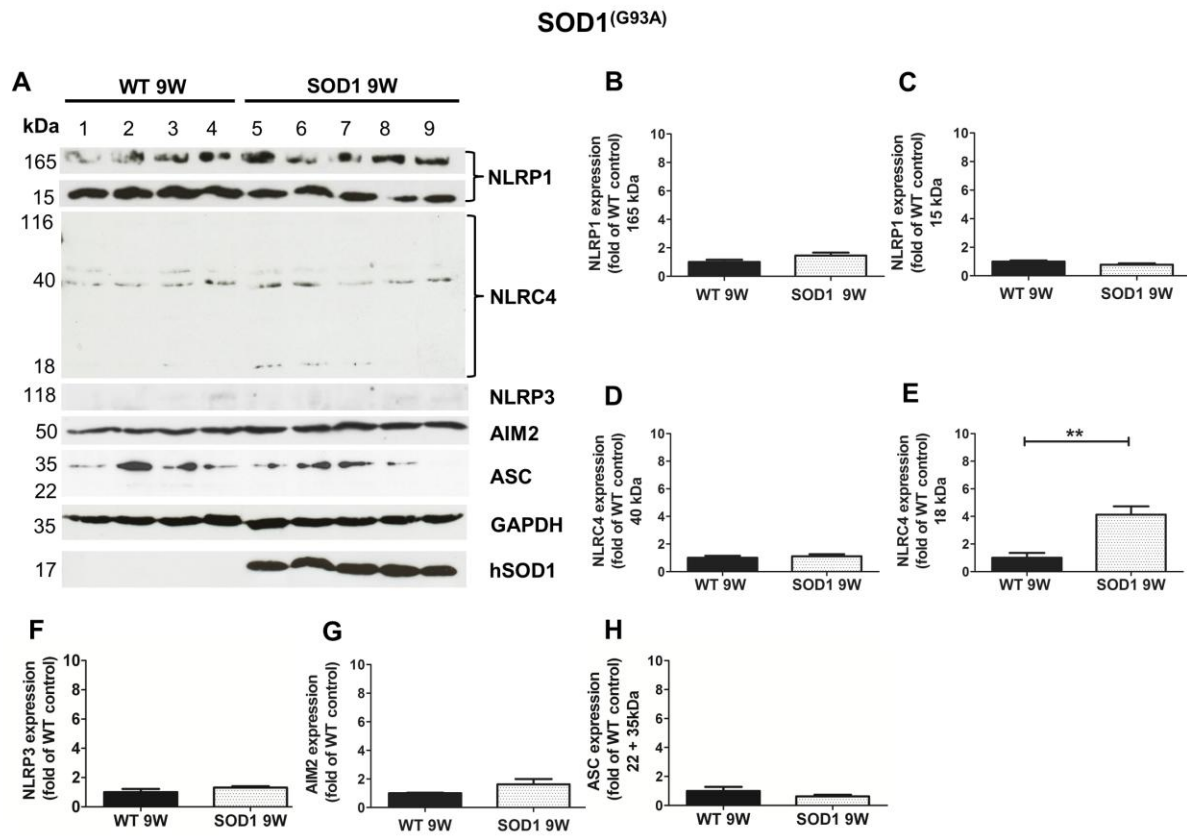


Figure 4

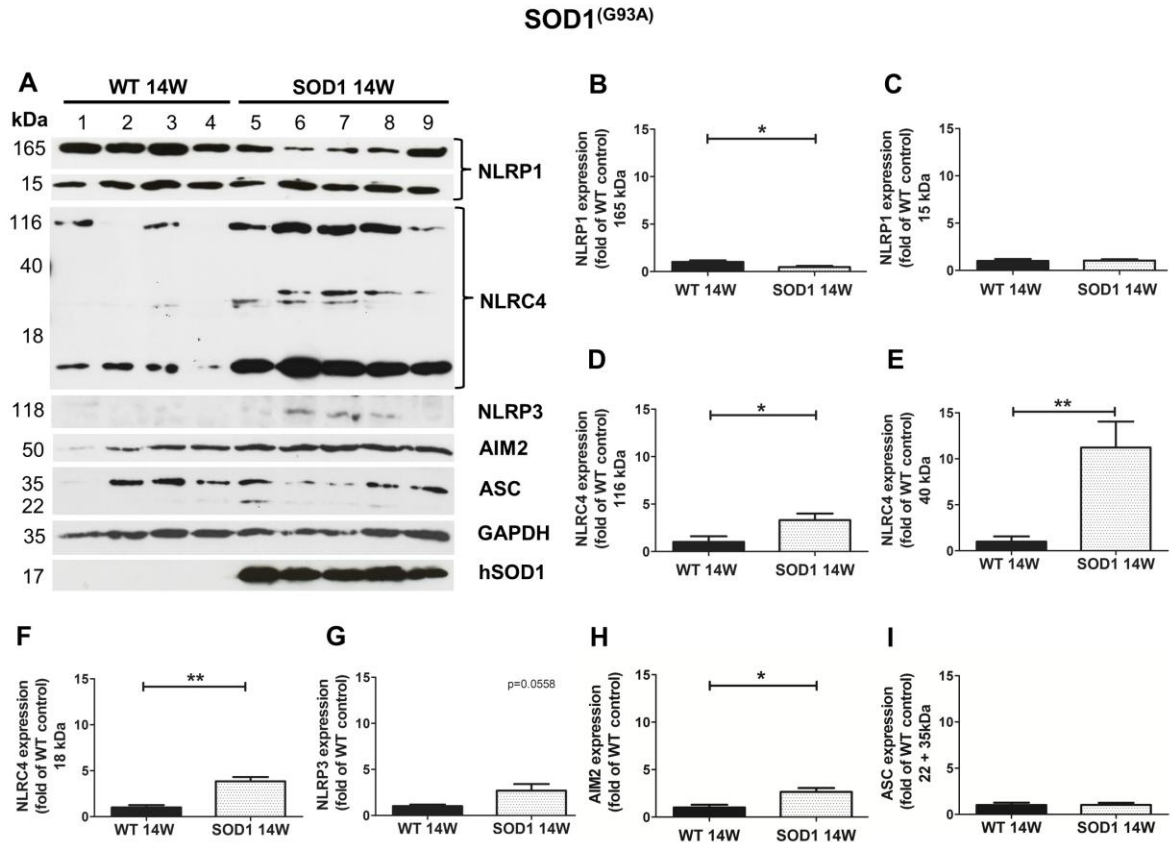


Figure 5

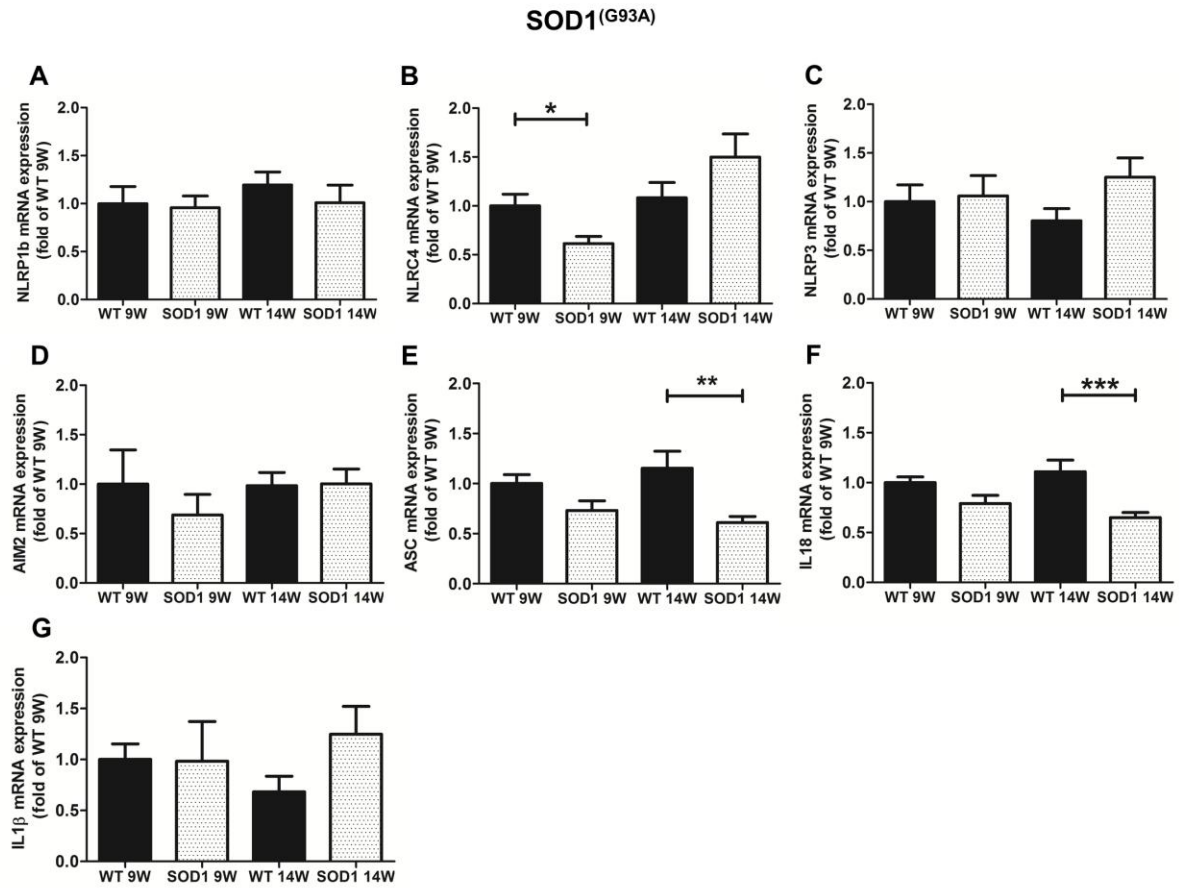


Figure 6

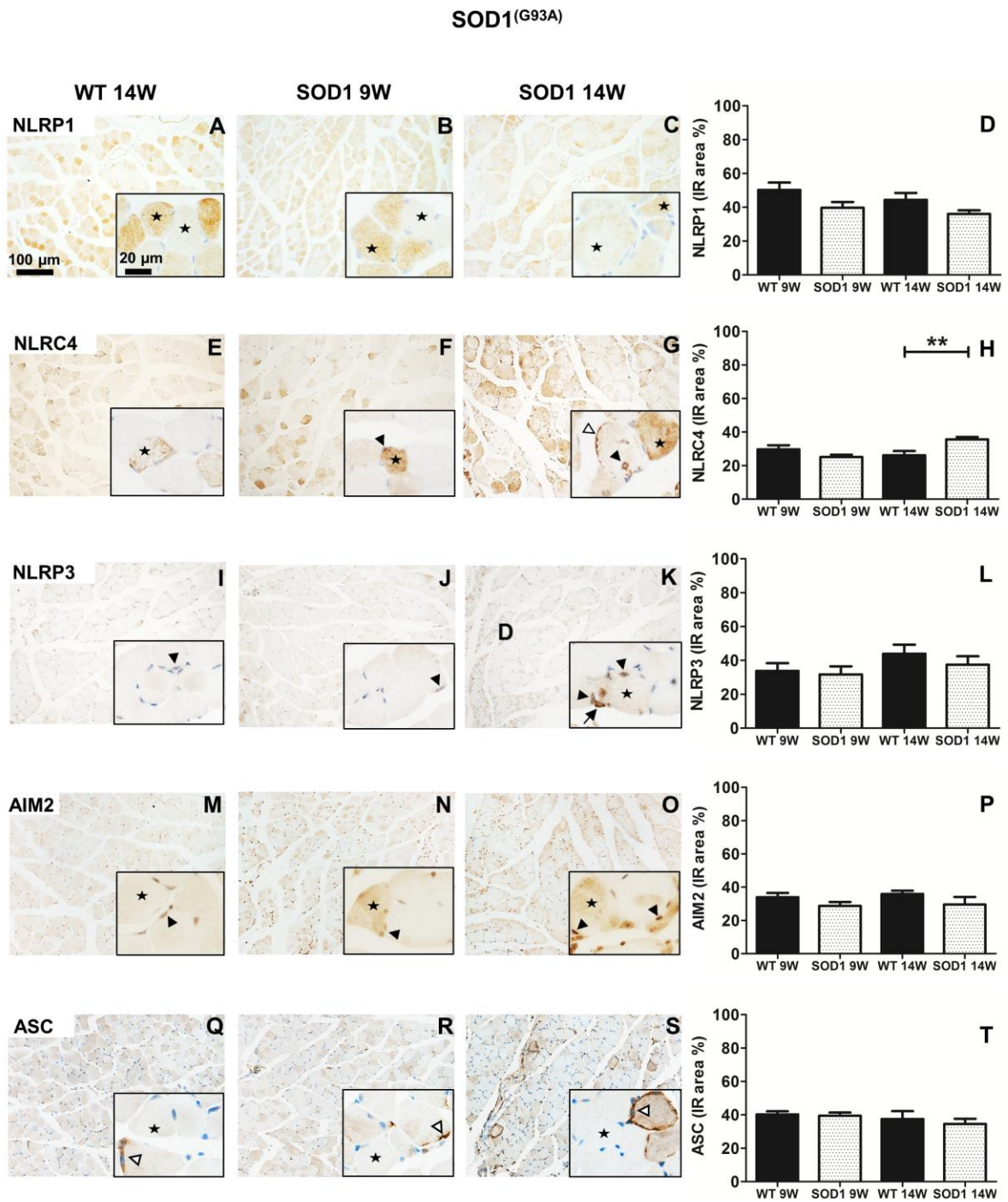


Figure 7

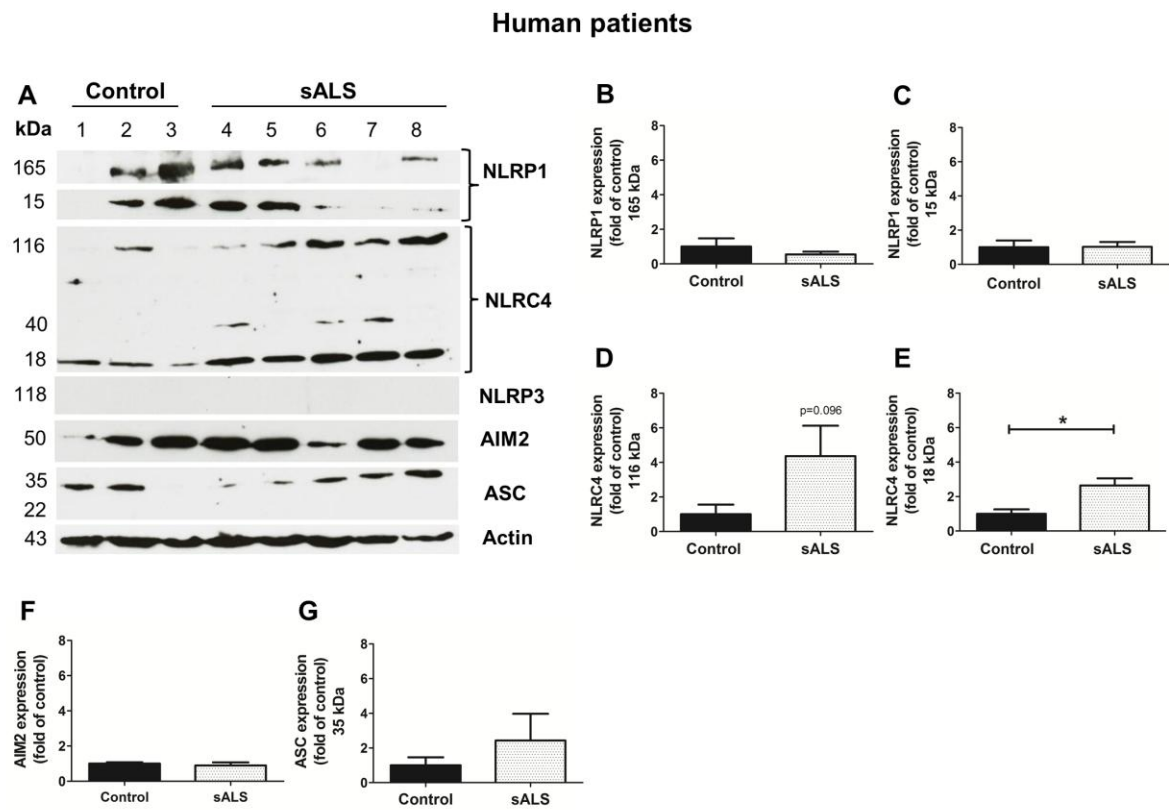


Figure 8

Human patients

